Metabotropic glutamate receptor activity induces a novel oscillatory pattern in neonatal rat hypoglossal motoneurones

Elina Sharifullina, Konstantin Ostroumov and Andrea Nistri

Neurobiology Sector and INFM Unit, International School for Advanced Studies (SISSA), Trieste, Italy

Tongue muscles innervated by the hypoglossal nerves play a crucial role to ensure airway patency and milk suckling in the neonate. Using a slice preparation of the neonatal rat brain, we investigated the electrophysiological characteristics of hypoglossal motoneurones in the attempt to identify certain properties potentially capable of synchronizing motor commands to the tongue. Bath-applied DHPG, a selective agonist of group I metabotropic glutamate receptors (mGluRs), generated persistent, regular electrical oscillations (4–8 Hz) recorded from patch-clamped motoneurones. Under voltage clamp, oscillations were biphasic events, comprising large outward slow currents alternated with fast, repeated inward currents. Electrical oscillations had amplitude and period insensitive to cell membrane potential, and required intact glutamatergic transmission via AMPA receptors. Oscillations were mediated by subtype 1 receptors of group I mGluRs (mGluR1s), and were routinely observed during pharmacological block of glycinergic and GABAergic inhibition, although they could also be recorded in standard saline. Simultaneous recordings from pairs of motoneurones within the same hypoglossal nucleus demonstrated that oscillations were due to their strong electrical coupling and were blocked by the gap junction blocker carbenoxolone. Pacing of slow oscillations apparently depended on the operation of K_{ATP} channels in view of the block by tolbutamide or glibenclamide. Under current clamp, oscillations generated more regular spike firing of motoneurones and facilitated glutamatergic excitatory inputs. These data suggest that neonatal motoneurones of the nucleus hypoglossus possess a formerly undisclosed ability to express synchronous electrical oscillations, unveiled by activation of mGluR1s.

(Resubmitted 18 November 2004; accepted after revision 15 December 2004; first published online 20 December 2004)
Corresponding author A Nistri: Neurobiology Sector and INFM Unit, International School for Advanced Studies (SISSA), Trieste, Italy. Email: nistri@sissa.it

In brain areas like the thalamus or the hippocampus, neuronal electrical oscillations represent a signalling process important to communicate and consolidate information within networks (Kirk & Mackay, 2003; Steriade & Timofeev, 2003). Since oscillations may differ in shape, frequency, regularity and phase distribution, it seems likely that distinct oscillatory activities reflect specific modalities of network signalling. Studying their origin and function therefore represents a useful approach to understand the computational properties of certain neuronal networks.

As far as motor systems are concerned, rhythmic activities are typically expressed by locomotor networks. The origin of motor rhythms is traditionally assigned to interneuronal circuits (Grillner *et al.* 1998), although further studies have reported that spinal motoneurones themselves can generate oscillations dependent on NMDA receptors (Schmidt *et al.* 1998) and propagated via gap junctions (Kiehn *et al.* 2000). Rhythmic activities are also expressed by brainstem neurones (Oyamada *et al.* 1999; Wu *et al.* 2001; Leznik *et al.* 2002; Rybak *et al.* 2003) and can be investigated using as a model hypoglossal motoneurones (HMs) which convey the sole motor output to tongue muscles. Thus, HMs express rhythmic motor commands in conjunction with functions like respiration, swallowing, mastication and vocalization (Jean, 2001). It is, however, uncertain whether HMs can generate intrinsic oscillations and if they do so, the functional impact of oscillations on motor output.

We have recently observed how selective activation of subtype 1 receptors belonging to group I metabotropic glutamate receptors (mGluR1s) facilitates glutamatergic excitatory inputs onto HMs of the neonatal rat brainstem (Sharifullina *et al.* 2004). Because this receptor

 DOI: 10.1113/jphysiol.2004.079509

subtype is largely expressed in the developing hypoglossal nucleus (Hay *et al.* 1999), it seems likely that it could play an important role in HM-dependent activities like respiration and milk suckling that are vital for the neonate. Because mGluR1s can stimulate the emergence of oscillations in forebrain networks (Whittington *et al.* 1995; Beierlein *et al.* 2000; Cobb *et al.* 2000; Hughes *et al.* 2002*b*), we wondered whether mGluR1-mediated rhythmic oscillations could be a strategy employed by the hypoglossal nucleus network to optimize its motor output.

The present study reports how mGluR1 activation can trigger HMs to generate intrinsic, persistent oscillations propagated amongst these cells via electrical coupling and paced by rhythmic activation of K_{ATP} channels. These oscillations made spike firing coherent and regular, thus suggesting they could represent an important process to express rhythmic, synchronized motor commands to the tongue.

Methods

Slice preparation

All experiments were done in accordance with the regulations of the Italian Animal Welfare act (DL 27/1/92 n. 116) following the European Community directives no. 86/609 and 93/88 (Italian Ministry of Health authorization for the local animal care facility in Trieste: D. 69/98-B), and approved by the local authority veterinary service.

Under deep urethane anaesthesia (2 g (kg body wt)$^{-1}$), I.P. injection) neonatal (1- to 6-day-old; P1–6) Wistar rats were decapitated, their brainstems dissected out and fixed to an agar block (Donato & Nistri, 2000). Transverse slices 200 μm thick were cut in ice-cold Krebs solution. After 1 h recovery at 32°C, slices were kept for at least 1 h at room temperature before recording.

Whole-cell patch recording

HMs were visualized within nucleus hypoglossus with an infrared video-camera, patched and recorded under voltage and current clamp mode. A few cells were also injected with neurobiotin through patch pipette (0.2% in intracellular solution) and processed for histology (Lape & Nistri, 2001). All electrophysiological recordings (in voltage or current clamp mode) were carried out as described before in detail (Sharifullina *et al.* 2004). For voltage clamp experiments HMs were clamped within the range of −60 to −70 mV holding potential to minimize the leak current at rest. For current clamping, cells were initially kept at their resting level of membrane potential without injecting intracellular current which was applied for certain tests only.

Analysis of a sample of cells voltage clamped with a Cs^+-filled pipette gave an average holding potential of -62 ± 1 mV (input resistance $= 148 \pm 8$ MΩ; $n = 62$), while for a pool of cells recorded with intracellular K^+ solution the corresponding holding potential was -67 ± 2 mV (input resistance $= 163 \pm 13$ MΩ; $n = 26$; $P = 0.35$ between cell groups). For double-patch recordings two neighbour cells were simultaneously patch clamped (average distance ≤ 30 μm). To elicit synaptic glutamatergic responses we electrically stimulated premotoneurones in dorsomedullary reticular column (DMRC; Cunningham & Sawchenko, 2000) as detailed earlier (Sharifullina *et al.* 2004). Single stimuli were applied at 10 s interval (0.1 ms, 10–100 V intensity). All electrophysiological responses were filtered at 3 kHz, sampled at 5–10 kHz, acquired and analysed with pCLAMP 9.0 software (Axon Instruments).

Solutions and drugs

The external solution for cutting and maintaining slices contained (mM): NaCl, 130; KCl, 3; $NaHPO_4$, 1.5; CaCl, 1; $MgCl_2$, 5; glucose 15 (315–320 mosm), and was continuously oxygenated with O_2 95%–CO_2 5%. In the recording chamber slices were superfused with gassed solution containing (mM): NaCl, 130; KCl, 3; $NaHPO_4$, 1.5; $CaCl_2$, 1.5; $MgCl_2$, 1; glucose 15 (315–320 mosmol l^{-1}), pH 7.4. Unless otherwise stated, all experiments were done in the continuous presence of bicuculline (10 μM) and strychnine (0.4 μM) to block GABA and glycine-mediated transmission (Donato & Nistri, 2000; Marchetti *et al.* 2002) so that glutamatergic effects could be observed in isolation. Patch pipettes contained (mM): KCl, 130; NaCl, 5; $MgCl_2$, 2; $CaCl_2$ 0.1; Hepes, 10; EGTA, 5; ATP-Mg, 2; GTP-Na, 1 (pH 7.2 with KOH, 280–300 mosmol l^{-1}). In about 50% of recordings K^+ was replaced with equimolar Cs^+. The pipette solution used for voltage clamp experiments often also contained QX-314 (300 μM) to block voltage-activated Na^+ currents and slow inward rectifier (I_h) (Marchetti *et al.* 2003) as indicated in the Results. In a group of experiments 20 mM BAPTA was added to patch pipette to buffer intracellular Ca^{2+}.

Drugs were applied via the recording saline (2–3 ml min^{-1} superfusion rate) with the exception of AMPA, which was applied by pressure pulses (10–50 ms; 6 p.s.i. pressure; 100 μM solution; once every 45 s to minimize desensitization) via a closely positioned puffer pipette as described before (Sharifullina *et al.* 2004). General reagents were of analytical grade. The following drugs were purchased from Tocris (Bristol, UK): 7-(hydroxyimino)cyclopropa[b]chromen-1a-carboxylate ethyl ester (CPCCOEt; selective antagonist for mGlu1 receptors), (*RS*)-3,5-dihydroxyphenylglycine (DHPG; selective agonist for group I receptors and equipotent on mGlu1 and mGlu5 subtypes), 2-methyl-6-(phenylethynyl)pyridine hydrochloride (MPEP; selective

antagonist for mGlu5 receptors); (*RS*)-α-amino-3-hydroxy-5-methyl-4-isoxazolepropionic acid (AMPA), 6-cyano-7-nitroquinoxaline-2,3-dione (CNQX), D-amino-phosphonovalerate (APV), *N*-(2,6-dimethylphenylcarbamoylmethyl) triethylammonium bromide (QX-314), 4-ethylphenylamino-1,2-dimethyl-6-methylaminopyrimidinium chloride (ZD 7288), glibencl-amide, apamin, (*aS*)-*a*-amino-3-[(4-carboxyphenyl)methyl]-3,4-dihydro-5-iodo-2,4-dioxo-1(2H)-pyrimid-inepropanoic acid (UBP 301; selective antagonist for kainate receptors), (+/−)-4-(4-aminophenyl)-1,2-dihydro-1-methyl-2-propylcarbamoyl-6,7-methylenedio-xyphthalazine (SYM 2206; selective antagonist for AMPA receptors), (2*S*)-3-[[(1*S*)-1-(3,4-dichlorophenyl)ethyl]amino-2-hydroxy-propyl](phenyl-methyl)phosphinic acid (CGP 55845; selective antagonist for $GABA_B$ receptors).

Bicuculline methiodide, 4-hydroxyquinoline-2-carboxylic acid (kynurenic acid), dihydro-β-erythroidine hydrobromide, atropine sulphate, 1,2-bis(2-amino-phenoxy)ethane-*N*,*N*,*N*′,*N*′-tetraacetic acid tetrapotassium salt (BAPTA), tolbutamide, strychnine hydrochloride, and carbenoxolone (disodium salt) were purchased from Sigma; tetrodotoxin (TTX) was purchased from Latoxan, and caesium chloride from Calbiochem. Full details about receptor specificity and concentrations of DHPG and antagonists on mGluR1s are given by Schoepp *et al.* (1999).

Data analysis

Cell input resistance (R_{in}) was measured as mentioned previously (Sharifullina *et al.* 2004) while cell capacitance was monitored on-line using pCLAMP 9.0 software. To estimate the strength of electrical coupling between cell pairs, rectangular pulses (±0.3 nA, 1000 ms) were applied to one cell under current clamp and responses recorded simultaneously from both cells: the coupling coefficient was then estimated from the ratio between the response of the stimulated cell and the one of its coupled neighbour (Long *et al.* 2004).

Each oscillatory cycle comprised a cluster of fast inward currents followed by a slow outward component. To quantify the oscillatory period we measured the time between the first fast discharge in each cycle and the first discharge in the following cycle. For each cell at least 50 cycles were measured and averaged. Analysis of all current responses (synaptic as well as oscillatory ones) was carried out using a template search protocol (pCLAMP 9.0) applied to at least 5-min-long consecutive records. For each cell, templates of various events (synaptic, oscillatory components, etc.) were obtained from electrophysiological records and checked for adequacy when compared with actual responses. Coefficient of variation (standard deviation/mean; CV) was expressed as a percentage value. Data for response rise and decay times were obtained from the 10–90% time interval of the response peak. To fit slow oscillatory outward currents we used the sum of two exponents with pCLAMP 9.0 software. To quantify oscillation periods from current clamp traces when oscillations were associated with intermittent firing, we used their fast Fourier transform obtained with pCLAMP 9.0 software. Whenever current clamp oscillations were accompanied by spikes or devoid of any spike activity, we instead used the standard template constructing protocol reported above to obtain period values.

To check cross correlation between two simultaneously recorded cells, standard cross-correlation analysis was performed using pCLAMP 9.0 for 1 s epochs. Linear regression analysis was carried out with Origin 6.1 (OriginLab Corporation, Northampton, MA, USA). Data are given as mean ± S.E.M. and n is the number of cells, unless otherwise indicated. Statistical significance was assessed with Student's paired or unpaired t test, applied only to raw data with parametric distribution; $P < 0.05$ was considered as significant.

Results

To optimize detection of oscillations, the present investigation employed maximally effective concentrations (25–50 μM) of DHPG (Sharifullina *et al.* 2004). The database of the present study comprises 274 visually identified HMs (an example of a neurobiotin-filled cell is in Fig. 1*A*), 139 of which were recorded with intracellular Cs^+ solution and 135 with intracellular K^+.

Repertoire of oscillatory activity evoked by DHPG

Under voltage clamp conditions, DHPG (25–50 μM) induced a slowly developing inward current (see Fig. 1*B*), which peaked at 2.2 ± 0.1 min ($n = 49$) from the start of the application. On average, on cells recorded with intracellular Cs^+ the DHPG current amplitude was −101 ± 5 pA ($n = 44$) regardless of the presence of oscillations. On cells recorded with intracellular K^+ solution, the DHPG current amplitude differed depending on the presence (−125 ± 11 pA; $n = 28$) or the absence (−73 ± 9 pA; $n = 12$; $P = 0.008$) of oscillations.

As the inward current developed, a complex series of electrical events appeared as exemplified in Fig. 1*B*. First, the DHPG inward current was accompanied by a series of fast discharges made up by rapid, inward deflections of stereotypic nature (see their expanded time course in Fig. 1*C* where the record segment indicated by the open horizontal bar in Fig. 1*B* is shown on a 10 times faster scale). This response component was transient and, after 5.6 ± 0.9 s, was replaced by a distinctive, persistent oscillatory pattern, with repetitive events of considerably larger amplitude. The transition from fast discharges to

slow oscillations is shown in Fig. 1*C*. To better separate the characteristics of fast discharges and slow oscillations, such responses are compared in Fig. 1*D* and *E*, respectively, on a much faster time base. Each slow oscillation cycle was biphasic (Fig. 1*E*) with an outward current (with respect to the steady-state level reached in the presence of DHPG; see dashed line) and an inward component predominantly inclusive of fast oscillations.

Slow oscillations were present in 60% of cells recorded with intracellular Cs^+ and in 58% of those recorded with intracellular K^+, indicating they were not due to the choice of the main intracellular cation. Hence, because we found no difference in the incidence of cells generating oscillations in relation to the intracellular electrode solution, data were pooled together. Eighty-six per cent of cells which developed slow oscillations also generated early fast discharges such as those of Fig. 1*D*. The frequency of their electrical oscillations was in the 4–8 Hz range. Fast Fourier transform of the slow outward component of these oscillations revealed a single peak corresponding to 6.5 ± 0.6 Hz ($n = 12$).

Temporal characteristics of oscillatory activity

Figure 2*A* and *B* shows examples of further analysis of the inward and outward components of slow oscillations (same cell as in Fig. 1). A typical outward component (Fig. 2*A*) had a bi-exponential time course as indicated in the inset to the top of Fig. 2*A* in which the average ($n = 216$ events) as well as the bi-exponentially fitted outward currents are compared. Note that the initial fast deflection was followed by a slower phase gradually waning and turning inward, thus leading to the onset of the next event.

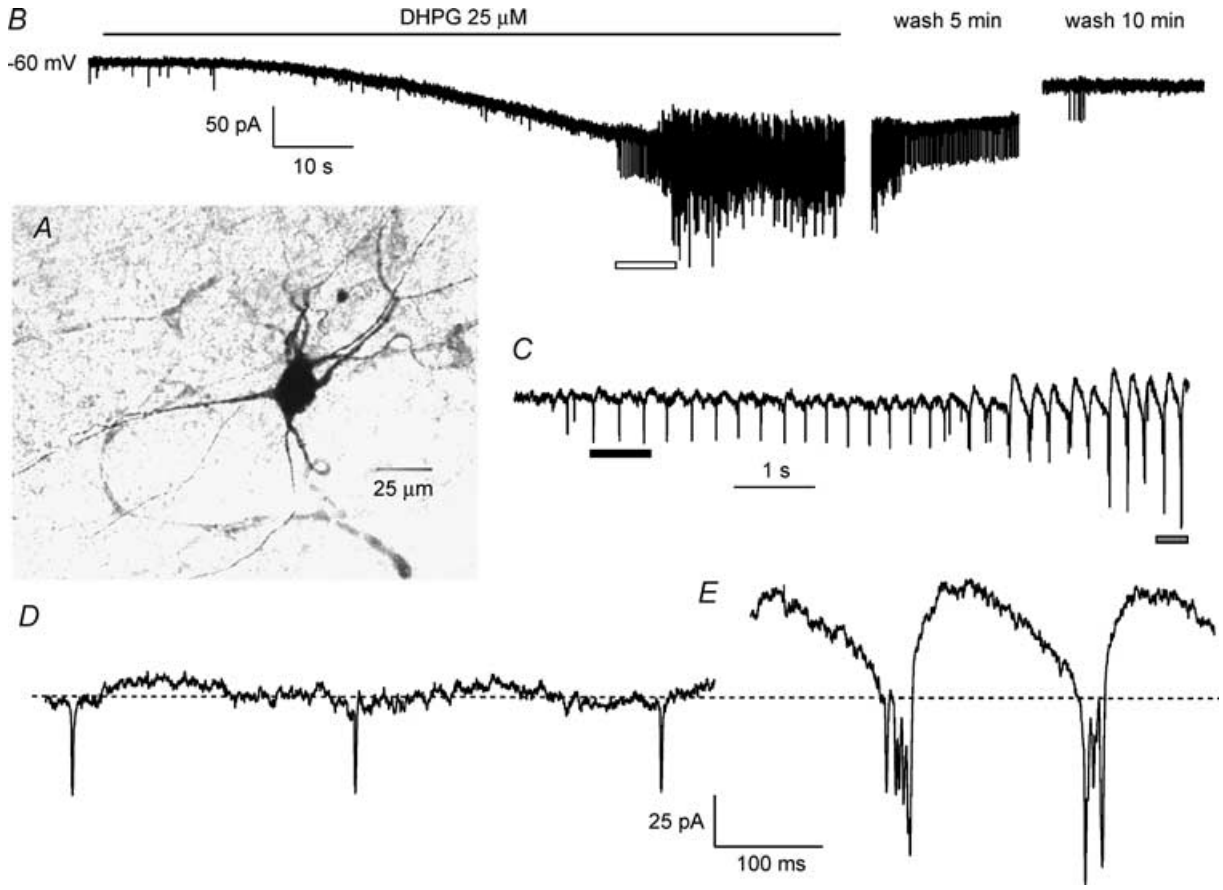

Figure 1. Oscillatory activity induced by DHPG on HMs
A, microphotograph of neurobiotin-filled neurone within the nucleus hypoglossus. Morphological features and size correspond to those of a HM. *B*, application of DHPG induces inward current and delayed appearance of oscillatory activity which gradually wanes after washout. *C*, faster time base records of trace indicated by open horizontal bar in *A* to show that the start of oscillatory activity comprises fast discharges and slow biphasic oscillations. Vertical calibration as in *B*. *D* and *E,* fast time base records of fast discharges and slow oscillations indicated in *C* by filled and shaded bars, respectively. Dashed line shows that slow oscillations include a large outward current (with superimposed synaptic currents) with respect to baseline attained between fast discharges. All data are from the same HM held at −60 mV.

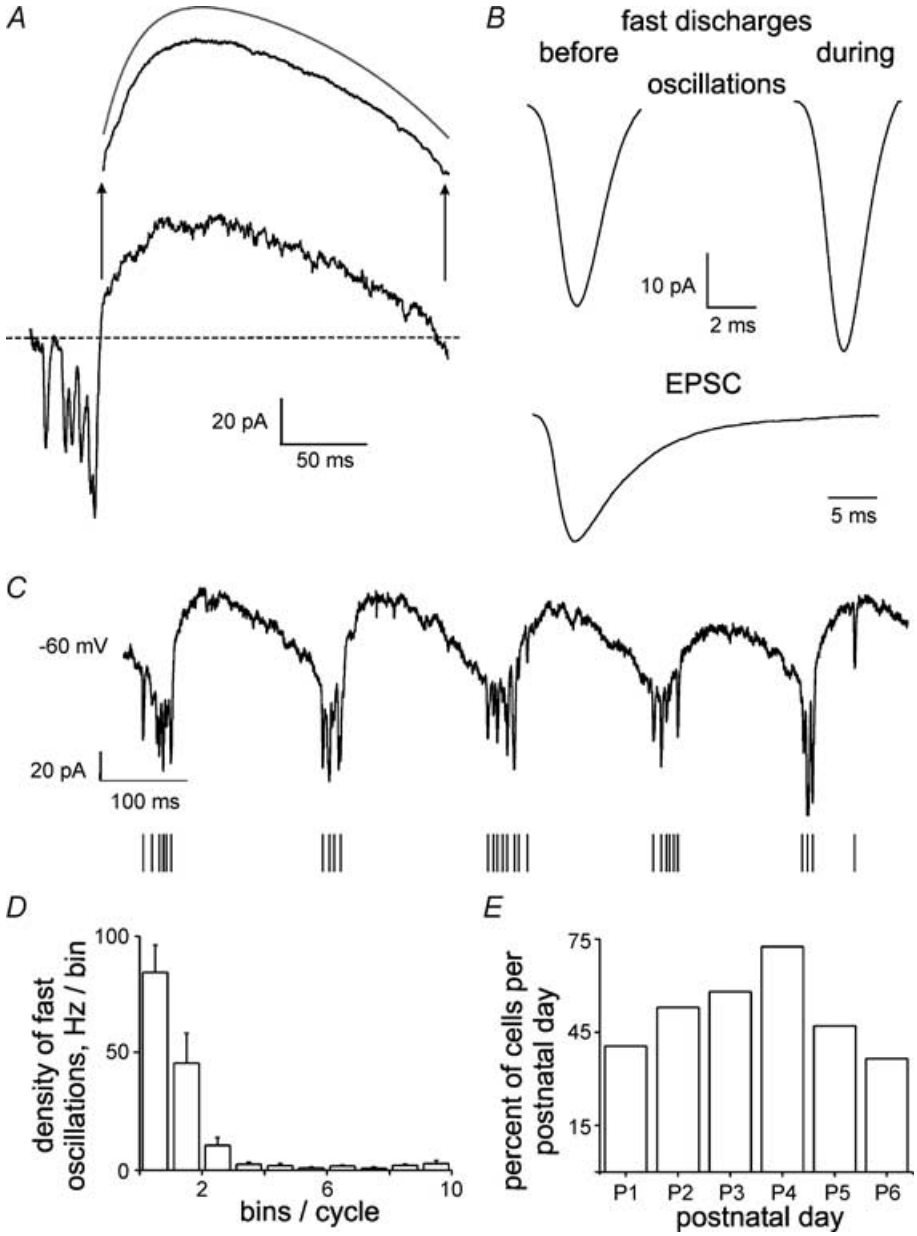

Figure 2. Characteristics of HM oscillations induced by DHPG
A, example of slow oscillation comprising repeated fast inward currents followed by a sustained outward current. The average outward component (216 events) is depicted above (see arrows) and can be well approximated by the sum of two exponents (top, grey). Note that synaptic events are superimposed on the outward currents Dashed line indicates baseline attained during application of 25 μM DHPG. *B*, average traces of fast inward discharges occurring before development of slow oscillations (left; see examples in Fig. 1*D*) or at the peak of each oscillations (see example in Fig. 1*E*). Their amplitude and time course are comparable; note, however, that these parameters are different from those of the average glutamatergic EPSC. All responses are from the same HM (further details in text); vertical bar applies to all three responses. *C*, tight relation between fast inward and slow outward currents during application of 25 μM DHPG. The occurrence of each fast inward current is indicated by a vertical bar below each cycle. *D*, plot of density of fast inward currents during the oscillatory cycle evoked by DHPG. For this purpose each cycle was divided into 10 bins (20.7 $\pm$ 2.7 ms bin time) and the number of fast inward current measured. Data are from 9 cells. Note clear clustering of fast inward currents at the start of each cycle. *E*, postnatal age-related occurrence of slow oscillations induced by DHPG. Maximum number of responsive HMs is at P4.

Table 1. Comparison of properties of oscillations and glutamatergic synaptic events of HMs in the presence of bicuculline and strychnine

	Amplitude (pA)	Rise time (ms)	Decay time (ms)	Periodicity	Period (CV, %)	*n*
Fast discharges	-47 ± 12	0.95 ± 0.08	2.06 ± 0.31	289 ± 78 ms	89 ± 39	9
Fast oscillations	-40 ± 4	0.98 ± 0.04	1.63 ± 0.11	15 ± 9 Hz	92 ± 50	13
EPSCs	-16 ± 2	1.38 ± 0.14†	5.62 ± 1.07*	2.6 ± 0.2 Hz	90 ± 18	8
Outward slow component	50 ± 3	18 ± 2	61 ± 8	154 ± 13 ms	24 ± 11	11

†$P = 0.01$ from fast discharges or fast oscillations; *$P = 0.0001$ from fast discharges or fast oscillations.

Inspection of the inward component (Fig. 2*A*) demonstrated multiple events of varying amplitude. Averaging 1255 such events from the same cell yielded a response of amplitude and time course very similar to those of the fast discharges ($n = 505$ events) preceding the slow oscillations. These events were therefore quite close in shape and amplitude (Table 1), suggesting that perhaps they had a common origin and could both be classified as fast discharges. Such discharges substantially differed from average spontaneous excitatory postsynaptic currents (EPSCs; Fig. 2*B*, $n = 1081$ events; Table 1).

We then examined, for slow oscillations, the temporal occurrence of fast oscillations within oscillatory cycles. This analysis is depicted in Fig. 2*C* and *D* in which, on the same HM, the number of fast oscillations was variable despite the regular periodicity of slow oscillations. It is, however, noteworthy that the number of fast oscillations in each event was always constrained between 2 and 10 for a very large sample of HMs ($n = 43$). Fast oscillations were usually clustered as shown by the histograms in Fig. 2*D* and typically occurred at 72 ± 8 ms ($n = 9$) before the peak of the slow outward component.

Conversely, when the temporal distribution of EPSCs was examined, it was apparent that the distribution of such events throughout the oscillation cycle was fitted by a simple Gaussian (not shown) with mean frequency of 2.6 ± 0.2 Hz ($n = 8$; Table 1), indicating that the probability of their occurrence was the same throughout the oscillation cycle.

Table 1 reports the basic properties of fast discharges and fast oscillations which were not significantly different in terms of amplitude, rise and decay times. These data thus strengthen the conclusions that these have a similar origin, and that they were clearly distinguishable from spontaneous EPSCs. The outward component of the slow oscillations was typically very regular in its periodicity (see low value of CV), unlike fast oscillations characterized by a very large CV value.

Predictors of slow oscillatory activity

Cells which generated slow oscillations had significantly larger cell capacitance (67 ± 4 pF, $n = 30$) than non-oscillatory cells (55 ± 3 pF, $n = 26$; $P < 0.009$).

Our previous observations about a significant input resistance increase evoked by DHPG (Sharifullina *et al.* 2004) were confirmed in the present study as long as HMs did not generate slow oscillations in the presence of DHPG (input resistance was augmented by $32 \pm 9\%$; $n = 25$; $P < 0.05$). When slow oscillations appeared, cell input resistance returned close to control values ($1 \pm 6\%$; $n = 33$) despite the continuous presence of DHPG.

Once slow oscillations were generated, their properties (amplitude, periodicity) were not dependent on the actual concentration of DHPG (25–50 μM or even 5 μM that could evoke oscillations in a minority of cells only), and persisted as long as the mGluR agonist was applied (our longest test was about 1 h). As shown in Fig. 1*B*, once DHPG was washed out, slow oscillations gradually disappeared, were replaced by fast discharges and finally any repetitive activity was absent while the baseline control level was re-attained. However, fast discharges and slow oscillations could be reproduced by a further application of DHPG (not shown).

Figure 2*E* shows that the chance of detecting slow oscillations was dependent on the preparation postnatal age. The incidence was highest at P4, falling before and after this age.

Voltage sensitivity of oscillatory activities

The complex nature of oscillatory behaviour induced by DHPG raised questions concerning the identification of such activities, their origin and underlying mechanisms. First, we used changes in holding potential to find out if oscillations were generated by a network process or were intrinsic to the recorded HM. Once the steady inward current induced by DHPG was at plateau, we shifted the membrane potential to values ranging from -100 to $+40$ mV. One representative experiment is shown in Fig. 3*A* in which the period of the slow oscillations was essentially unchanged at three different levels of holding potential. Furthermore, slow oscillations could not be reversed even at very positive values of holding potential ($+40$ mV), although some slow, long outward responses were present (see example in Fig. 3*A*). Similar data were obtained by applying slow voltage ramps from -100 to $+60$ mV (not shown). Figure 3*B* shows that there was no

significant change in periodicity, amplitude of the slow oscillations and amplitude of the fast oscillations within the −100–0 mV range. Note that, in the absence of DHPG, analogous voltage shifts did not produce slow oscillations, although fast discharges could be observed between −40 and 20 mV in the presence of intracellular Cs^+ ($n = 25$; not shown).

We identified the slow, long outward currents intermittently appearing at +40 mV as reversed EPSCs as shown in Fig. 4 (see asterisks). In this cell that developed standard oscillations in the presence of 25 μM DHPG, we set the membrane potential at +40 mV and applied a combination of selective blockers for kainate receptors (10 μM UBP 301; More *et al.* 2003), NMDA receptors (50 μM APV) and $GABA_B$ receptors (10 μM CGP 55845; Towers *et al.* 2002) which did not block the generation of such slow, irregular outward currents (Fig. 4*A*). Full persistence of this activity was observed in seven cells. However, application of the selective AMPA receptor blocker SYM 2206 (10–30 μM; Behr *et al.* 2002) fully abolished the large outward currents while leaving the fast inward discharges. These data suggest the large, irregular outward currents were due to activation of AMPA-sensitive receptors by endogenously released glutamate (Fig. 4*B*; similar data were obtained from 4 cells).

The behaviour of the spontaneous reversed EPSCs was further explored in experiments like the one depicted in Fig. 5 which, for the sake of avoiding complications due to the concomitant occurrence of oscillations, shows responses from a HM not oscillating in DHPG solution (pipette filled with Cs^+ and QX-314). In this case, DHPG also produced a slowly developing inward current as exemplified in Fig. 5*A* associated with increased occurrence of spontaneous EPSCs. We then applied slow

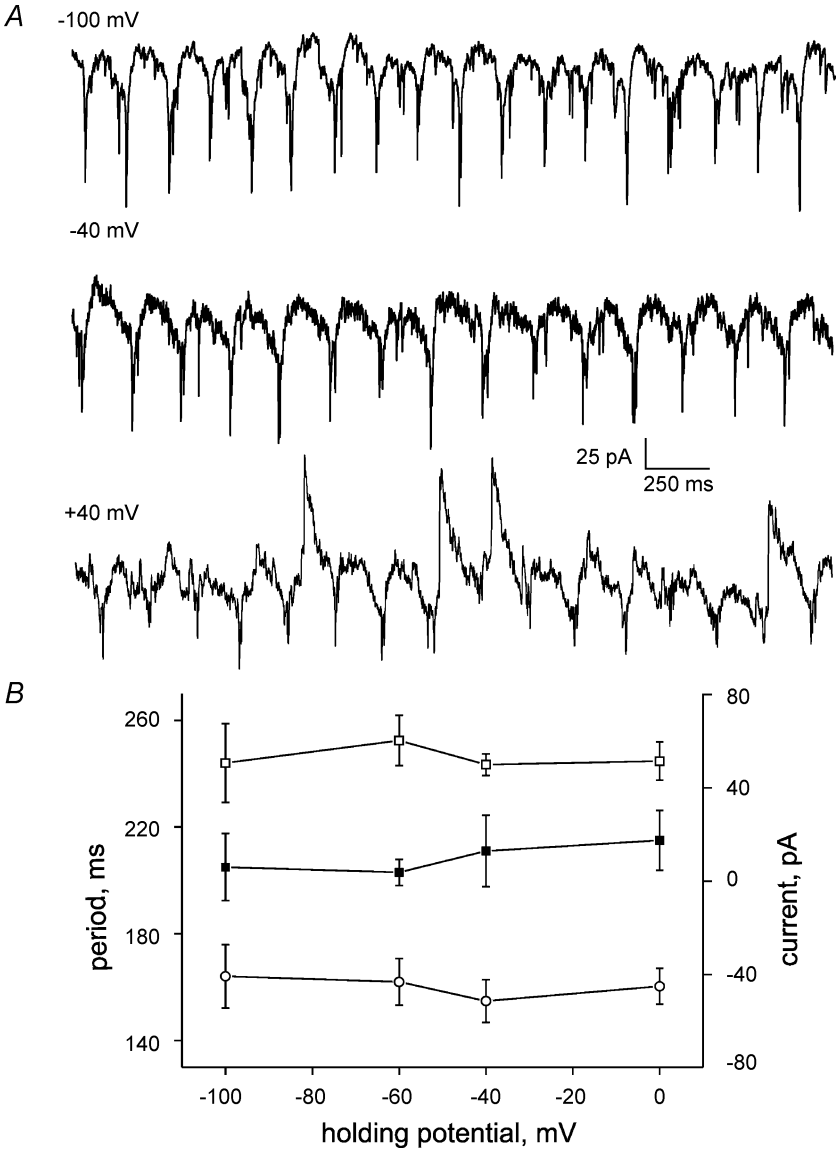

Figure 3. Voltage sensitivity of oscillations evoked by DHPG
A, sample records of oscillations recorded at three different levels of membrane potential (values indicated above each record) of the same HM. Patch pipette contained QX-314 (300 μM) to inhibit voltage-dependent Na^+ and I_h currents. Note relative insensitivity of oscillation period and amplitude to membrane potential. At +40 mV random outward events are reversed EPSCs. *B*, average plots of amplitude of oscillation outward currents (□; right vertical scale), oscillation period (■; left vertical scale), and amplitude of oscillation inward currents (○; right vertical scale). Values are from 9 cells recorded with QX-314-filled electrodes.

changes in the holding potential from −60 to +40 mV (see bottom trace in Fig. 5*A*) that fully reversed the irregular discharges which acquired a much slower decay phase (54 ± 7 *versus* 191 ± 13 ms time constant; see inset to Fig. 5*A*, comparing average currents at the two different holding potentials). Additional corroboration of the distinctive voltage sensitivity of AMPA receptor-mediated currents was obtained by examining the behaviour of currents elicited by puffer application of AMPA in a solution containing (in addition to strychnine and bicuculline) 10 μM UBP 301, 50 μM APV and 1 μM TTX. Figure 5*B* shows that both the peak amplitude as well as the area of the AMPA-evoked currents displayed outward rectification as their size grew at positive membrane potential.

Merely raising extracellular K^+ to 7.5–9 mM evoked a large inward current (-125 ± 15 pA; $n = 7$), enhanced EPSC frequency, yet failed to induce fast discharges and slow oscillations.

Pharmacology of oscillatory activity

A number of studies of brain slice neurones have shown that periodic oscillations can be generated (or modulated) by certain voltage-activated ionic channels, including those permeable to Na^+, or Ca^{2+}, or with Ca^{2+}-dependent K^+ permeability, as well as slow inward rectifiers (Traub *et al.* 2002, 2004).

Fast discharges and slow oscillations were routinely observed in DHPG solution when cells were recorded with an electrode containing the sodium current and I_h blocker QX-314 (Marchetti *et al.* 2003; $n = 56$ out of 92; 61%; see example in Fig. 3*A*). Likewise, the full range of oscillatory activity was detected in cells recorded with the Ca^{2+} buffer BAPTA (20 mM plus 5 mM EGTA; 11 out of 17 cells; 65%). Oscillatory activity induced by DHPG was not affected in the presence of extracellular Cs^+ (2–3 mM) and/or the I_h inhibitor ZD 7288 (20 μM; $n = 12$), Ba^{2+} (2 mM; $n = 5$) or apamin (100 nM; $n = 9$).

Omission of strychnine and bicuculline from the extracellular solution manifests large spontaneous postsynaptic inhibitory currents on HMs because the most conspicuous on-going activity is generated by network-dependent release of GABA and glycine (Donato & Nistri, 2000) rather than glutamate (Sharifullina *et al.* 2004). In the present experiments we could observe repeated oscillatory activity evoked by DHPG on nine HMs bathed in saline lacking bicuculline and strychnine. However, in three cells only, the oscillatory activity was not largely contaminated by intense inhibitory synaptic currents which are strongly facilitated by mGluR agonists (Donato & Nistri, 2000). On such cells, systematic analysis of their DHPG-evoked oscillatory activity showed it similar (Table 2) to the one recorded following pharmacological block of synaptic inhibition (see Table 1). Thus, inhibitory receptor antagonists were not a prerequisite to detect oscillations, rather they optimized the experimental conditions to analyse them.

In the presence of cholinergic antagonists (20 μM atropine, 50 μM dihydro-β-erythroidine; $n = 3$), or in the presence of APV (50 μM; $n = 5$), oscillatory activity was unaffected.

At standard holding potential, kynurenate (2 mM; $n = 14$), or CNQX (20 μM; $n = 6$) always blocked the DHPG (25 μM)-evoked slow oscillations as indicated in the example of Fig. 6*A* for a CNQX experiment. In the

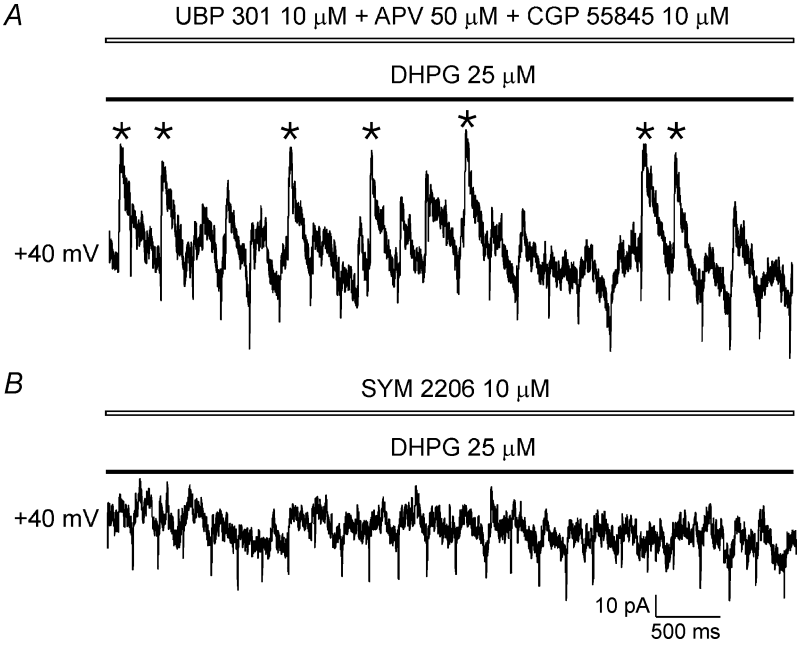

Figure 4. Slow, large outward currents during DHPG application to depolarized HMs are due to AMPA receptor activity
A, after initial application of DHPG (25 μM) that generated typical oscillations, the cell holding potential is shifted to +40 mV in the continuous presence of the kainate blocker UBP 301, the NMDA blocker APV and the $GABA_B$ antagonist CGP 55845. Note that large, slow currents (indicated by asterisks) persist. *B*, on the same cell shown in A, further application of the AMPA receptor antagonist SYM 2206 suppresses the slow, large outward currents.

continuous presence of CNQX or kynurenate plus DHPG, depolarizing the membrane potential by either holding it at a constant depolarized level (0 mV in the example of Fig. 6*A*) or applying a voltage ramp (not shown), could, however, evoke fast discharges. Slow oscillation recovery was attained after washout of CNQX (Fig. 6*A*). Analogous data were obtained with the selective AMPA receptor antagonist SYM 2206 (10 μM; $n = 4$; not shown). To confirm the involvement of ionotropic glutamate receptors in slow oscillations, puffer applications of AMPA were delivered in control conditions (Fig. 6*B*) and after applying a concentration of DHPG (5 μM) which was subthreshold to generate oscillations (Fig. 6*B*). In the presence of DHPG, the peak amplitude of the AMPA-induced inward current was increased ($21 \pm 6\%$; $n = 5$; Sharifullina *et al.* 2004), and was associated with strong oscillatory activity (4 out of 5 cells) reversible on washout. Figure 7 shows that the combined action by AMPA and DHPG in promoting oscillatory activity did not require activation of kainate receptors. In fact, in the continuous presence of the kainate antagonist UBP 301 (10 μM), DHPG generated an inward current (see downward shift in baseline) and enabled AMPA (applied by the puffer pipette) to elicit repeated oscillations after the peak inward current response (Fig. 7*A*). Similar data were obtained from four cells. It is noteworthy that 10 μM UBP 301 *per se* did not significantly affect the peak amplitude of AMPA-induced currents ($94 \pm 8\%$; $n = 4$) nor did it change the oscillatory pattern evoked by 25 μM DHPG ($n = 4$). On the other hand, in the presence of the selective AMPA receptor blocker SYM 2206 (10 μM), despite the inward current generation by DHPG, AMPA responses

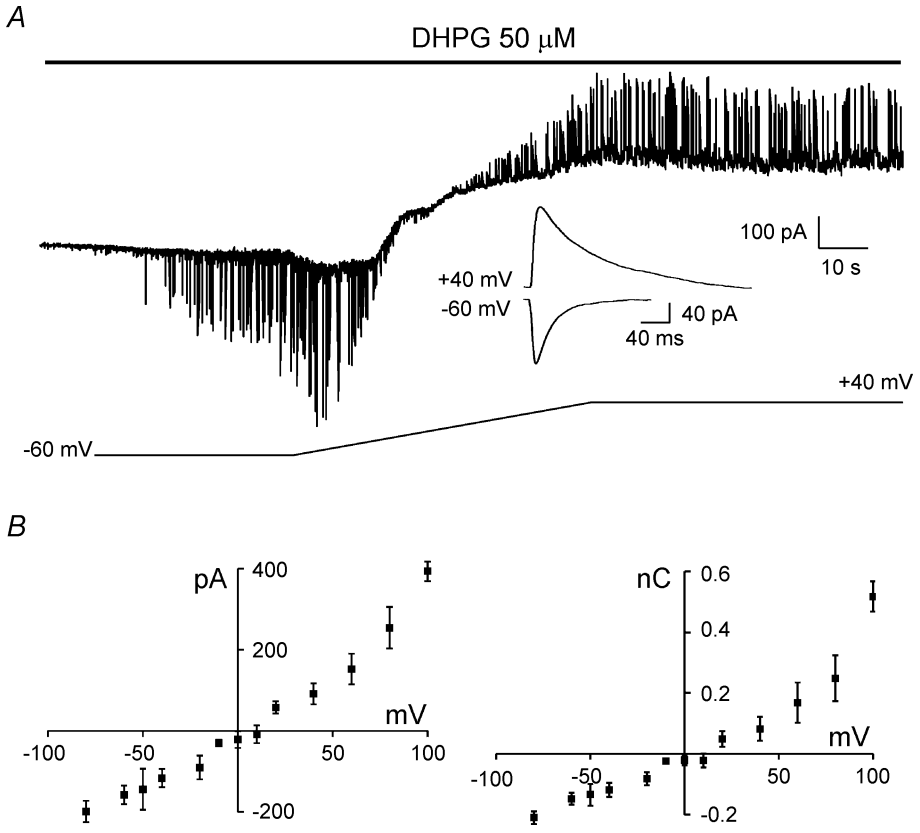

Figure 5. Rectification of AMPA receptor mediated responses of HMs
A, application of DHPG (50 μM) evokes a slowly developing inward current without associated oscillations on this cell, but it strongly facilitates spontaneous inward glutamatergic currents which reverse polarity once the cell is slowly depolarized to +40 mV (see scheme of the voltage change below the current trace). The inset shows that the average synaptic outward current (100 events) at +40 mV has different kinetics from the corresponding average current (112 events) recorded at −60 mV. Application of the slow voltage ramp protocol evokes a non-linear behaviour of whole membrane current probably due to activation of voltage-dependent conductances of the recorded HM. Bathing solution contained 10 μM bicuculline and 0.4 μM strychnine only. *B*, plots of mean peak amplitude and area of currents evoked by puffer application of AMPA to HMs in the presence of 1 μM TTX, 10 μM UBP 301 and 50 μM APV (plus bicuculline and strychnine) and recorded at different holding potentials. Note that the amplitude and, particularly, the area of the response grows non-linearly at positive potentials. Data are from 4 cells.

Table 2. Properties of DHPG induced oscillations of HMs recorded in the absence of bicuculline and strychnine

	Amplitude (pA)	Rise time (ms)	Decay time (ms)	Periodicity	Period (CV, %)	*n*
Fast discharges	-60 ± 12	1.12 ± 0.16	2.12 ± 0.45	250 ± 103 ms	97 ± 38	3
Fast oscillations	-33 ± 15	0.85 ± 0.14	1.71 ± 0.20	18 ± 8 Hz	72 ± 25	3
Outward slow component	40 ± 13	23 ± 5	76 ± 11	127 ± 15 ms	50 ± 2	3

were largely attenuated to 21 ± 4% of control ($n = 3$) and failed to be associated with oscillations (Fig. 7*B*; same cell as in Fig. 7*A*).

Application of TTX (1 μM) via the bathing solution always eliminated slow oscillations and prevented appearance of fast discharges upon membrane depolarization ($n = 10$). Likewise, adding the inorganic Ca^{2+} antagonist Mn^{2+} (2 mM; $n = 6$) rapidly blocked slow oscillations and fast discharges, an effect which was reversible within 15 min washout of this divalent cation. The action of DHPG was blocked by application of the selective mGluR1 antagonist CPCCOEt (100 μM; $n = 7$), and unaffected by the selective subtype 5 blocker MPEP (40 μM; $n = 6$) (data not shown).

Collectively, these data suggest that, at network level, combined activation of both mGluRs and AMPA receptors created the conditions to generate slow oscillations.

Electrical coupling amongst HMs is essential for oscillatory activity

Previous studies have identified electrical coupling between brainstem motoneurones under *in vivo* and *in vitro* conditions (Mazza *et al.* 1992; Rekling *et al.* 2000). Since electrical coupling can be responsible for oscillatory activity in other brain areas (Galarreta & Hestrin, 1999; Landisman *et al.* 2002; LeBeau *et al.* 2003), it was important to ascertain whether this process was influencing oscillations of HMs. For this purpose we performed simultaneous patch clamp recording from pairs of HMs (within the same nucleus hypoglossus). Fourteen pairs were thus recorded, of which six (43%) were electrically coupled with a coupling coefficient of 0.039 ± 0.008 for depolarizing current and 0.049 ± 0.012 for hyperpolarizing current, indicating lack of significant rectification ($P > 0.05$). An example of two electrically coupled HMs is shown for control conditions in Fig. 8*A* in which one cell was under voltage clamp (cell 1, top) and the other one under current clamp (cell 2, bottom). Application of a depolarizing (left) or hyperpolarizing (right) current pulse to cell 2 elicited in cell 1 an inward or an outward current, respectively (the latter followed by an off-response in either cell). Note that, during repeated firing of cell 2, cell 1 displayed fast inward discharges locked 1 : 1 with spikes as indicated by the cross-correlation plot. Thus, fast discharges could be identified as 'spikelets' (Perez Velazquez & Carlen, 2000; Hughes *et al.* 2002*a*; Long *et al.* 2004).

Figure 8*B* (same cell as in Fig. 8*A*) shows that, in the presence of DHPG (25–50 μM), cell 2 exhibited regular spiking activity associated (on a 1 : 1 basis) with slow oscillations resembling 'burstlets' (Long *et al.* 2004). The peak of each action potential of cell 2 coincided with the peak of spikelets in cell 1, while the interspike interval (ISI) was associated with burstlets. The strong association between spikes and spikelets as well as ISIs and burstlets is shown in the plot of Fig. 8*B*. Pooling data from all paired cells oscillating in the presence of DHPG gave a coupling coefficient of 0.028 ± 0.0005, that was not significantly different ($P = 0.33$) from control.

Confirmation of the dependence of oscillations on electronic coupling amongst HMs was obtained by applying the gap junction blocker carbenoxolone (100 μM; $n = 6$) as demonstrated in Fig. 8*C* (same pair of cells as in Fig. 8*A* and *B*). After 12 min application of this drug, full suppression of spiking in cell 2 and slow oscillations in cell 1 became apparent. Furthermore, in the continuous presence of DHPG and carbenoxolone, a large depolarizing pulse (0.6 nA) applied to cell 2 elicited spikes in the same cell, yet it failed to generate a current response in cell 1. Further evidence for electrotonic coupling between such cells was also demonstrated by applying a large hyperpolarizing current to cell 2 to suppress its spike activity during application of DHPG, although oscillations persisted even at -76 mV membrane potential (Fig. 8*D*). This manoeuvre was associated with a clear slowing down of slow oscillations in cell 1 and subsequent recovery after injection of current into cell 2 was terminated (Fig. 8*D*). In the presence of carbenoxolone the coupling coefficient amongst cells was severely reduced (0.0015 ± 0.00003; $n = 6$).

Figure 8*E* and *F* shows examples of other responses recorded from pairs of cells during application of DHPG. In Fig. 8*E* both cells were generated slow oscillations and regular spiking, although at different frequencies and thus uncorrelated as shown by the corresponding correlogram ($n = 2$ pairs). In Fig. 8*F*, one cell was not oscillating while the other one was spiking regularly ($n = 2$ pairs). In all these cases application of carbenoxolone disrupted bursting indicating that, although within these

pairs cells were not coupled, they were presumably coupled to other neurones to support their oscillatory activity.

Experiments with carbenoxolone were also carried out on single-recorded HMs ($n = 9$) in which full suppression of slow oscillations was observed despite the persistence of the inward current induced by DHPG (not shown).

K_{ATP} conductance as pacer of slow oscillations

Because various pharmacological blockers acting on disparate voltage-activated conductances failed to suppress the DHPG-induced slow oscillations, the question of the identity of the mechanisms responsible for the large outward currents inherent in each oscillatory cycle remained unanswered. Recent studies have suggested that some brainstem respiratory neurones possess a K_{ATP} conductance which controls their rhythmic bursting because their intracellular ATP is metabolically consumed and thus the block of the K^+ channels is transiently removed (Haller *et al.* 2001). The rapid cycle of ATP generation and consumption would then be a major contributor for setting the respiratory rhythm frequency (Haller *et al.* 2001).

We examined if an analogous mechanism might have been applicable to HMs oscillating in the presence of DHPG. To this end, we applied two known K_{ATP} blockers, namely glibenclamide (50 μM) and tolbutamide (500 μM). Figure 9*A* exemplifies one such experiment. Typical slow oscillations were evoked by bath-applied DHPG (25 μM; filled horizontal bar; see also left inset to Fig. 9*A* with expanded time scale). Subsequent application of tolbutamide (open horizontal bar) induced a further slow inward current and disruption of slow oscillatory activity, while less regular (CV = 36% *versus* 8% prior to tolbutamide) fast discharges survived (see middle inset to Fig. 9*A*). Washing out tolbutamide in the continuous presence of DHPG restored the baseline current to the level attained during the oscillatory activity and regenerated typical oscillations. Similar effects were observed on HMs bathed in glibenclamide ($n = 10$) or tolbutamide ($n = 7$) solution, although the blocking action by glibenclamide could not be reversed on washout, in accordance with its known irreversible block of K_{ATP} channels (Ashcroft, 1988). The steady inward current induced by glibenclamide or tolbutamide was essentially the same in amplitude so that data for the two treatments were pooled and gave an average magnitude of -57 ± 9 pA.

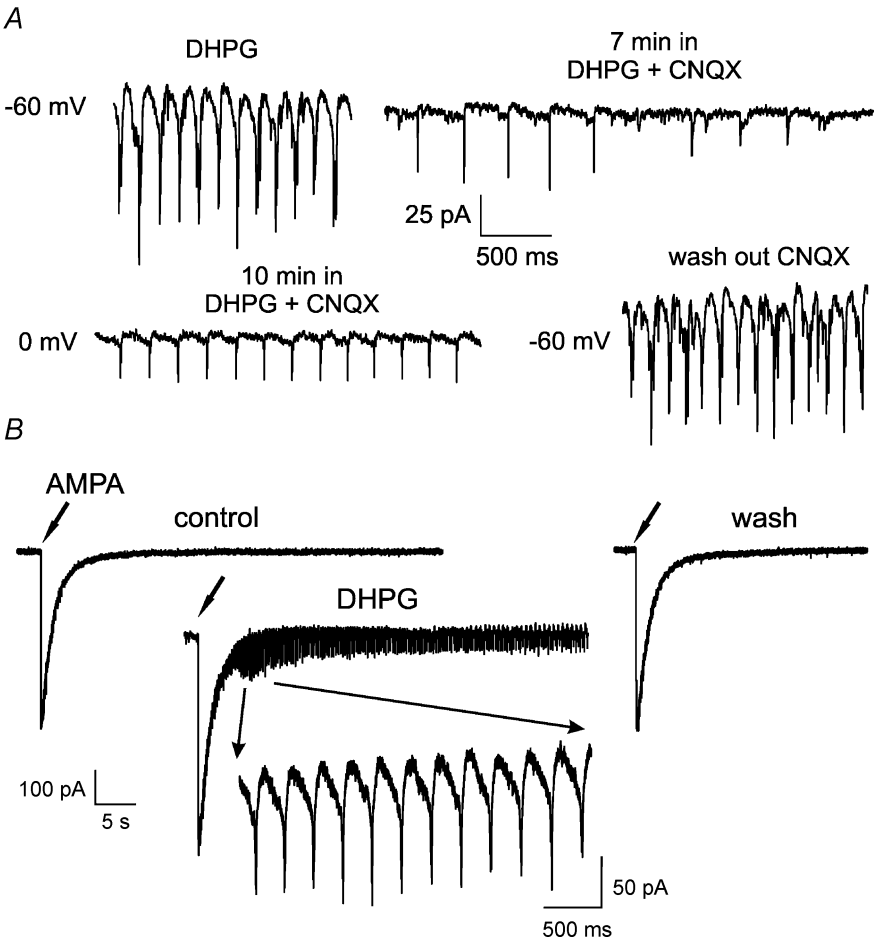

Figure 6. Block or activation of AMPA receptors depresses or facilitates oscillations evoked by DHPG
A, oscillations recorded at steady-state level in 25 μM DHPG solution (left, top) are disrupted by 20 μM CNQX, a blocker of AMPA/kainate receptors (right, top). This treatment leaves sporadic fast discharges only. Depolarization to 0 mV regenerates fast inward currents in the continuous presence of DHPG plus CNQX, although slow oscillations are absent (left, bottom). Washout of CNQX restores slow oscillations after 15 min at −60 mV (right, bottom). All records are from the same HM. *B*, puffer application of AMPA (see arrows) elicits inward current in control condition at −60 mV membrane potential (left). When the same application is repeated in the presence of a low concentration of DHPG (5 μM) subthreshold for oscillations, slow oscillations appear during the decay phase of the AMPA response (middle). This effect is reversible on washout of DHPG (right).

Figure 9*B* shows average *I–V* plots (achieved with voltage ramp protocols) obtained from cells ($n = 12$) during oscillations in the presence of DHPG (■) and their subsequent block by tolbutamide or glibenclamide (□). To aid comparison, the steady baseline current elicited by the sulphonylureas was subtracted from each curve. It is apparent that in the presence of sulphonylureas the average *I–V* relation was shifted downwards at all tested levels of membrane potential. Figure 9*C* (current scale larger than in Fig. 9*B*) shows that, in the range negative to the holding potential, the reduced slope of the plot in the presence of sulphonylureas led to an extrapolated crossover at −106 mV, namely close to the calculated K^+ reversal potential (−98 mV).

The effects of tolbutamide or glibenclamide on HMs were also investigated in current clamp experiments. Pre-incubation (20–60 min) in glibenclamide solution always prevented oscillatory activity by subsequent administration of DHPG, even if the DHPG-evoked depolarization had similar amplitude (12 ± 1 mV; $n = 5$ cells) as in control solution (14 ± 2 mV; $n = 35$; $P > 0.05$). On two HMs under current clamp, after full onset of slow oscillation in the presence of DHPG, subsequent application of tolbutamide (which induced an average 11 ± 2 mV depolarization) suppressed oscillations fully and reversibly. Collectively, these data therefore demonstrate that the ability of sulphonylureas to disrupt oscillations could be observed under voltage as well current clamp conditions.

HM firing characteristics during oscillations induced by DHPG

Experiments in current clamp conditions were performed to find out whether slow oscillations evoked by DHPG conferred certain properties to the cell's ability to fire action potentials. First, we compared cells which, in the presence of DHPG, did not oscillate with those that did (see example in Fig. 10*A*). At comparable level of membrane potential, a non-oscillating neurone (top

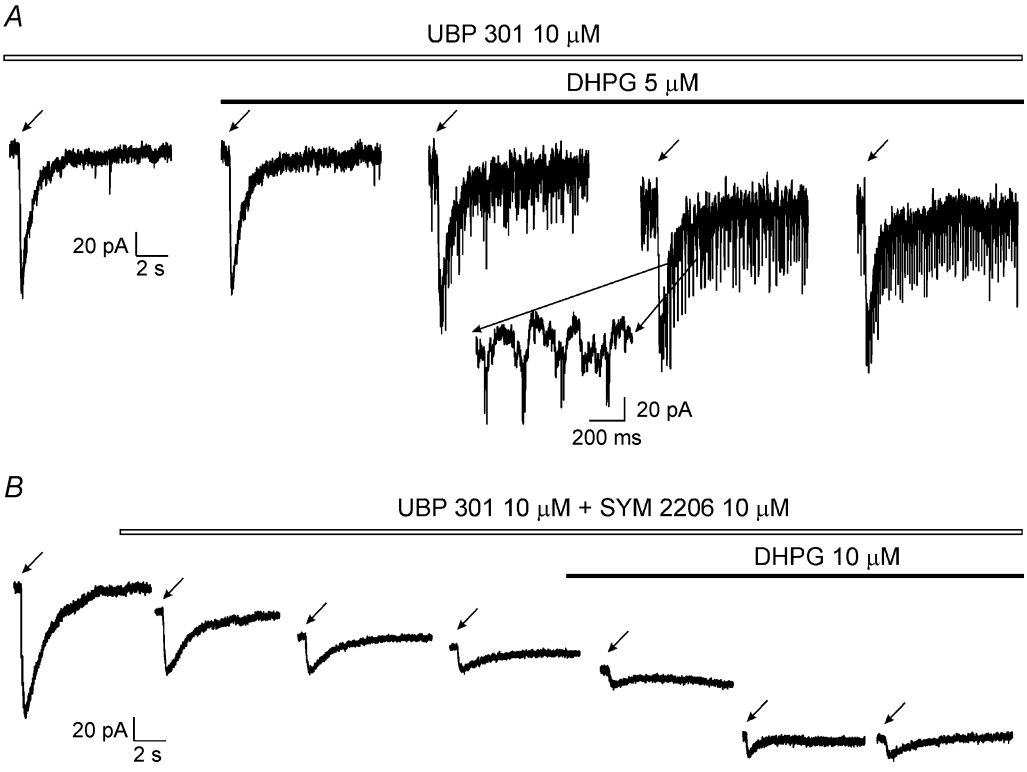

Figure 7. Synergic activation of oscillatory activity by AMPA and DHPG does not require kainate receptor activation

A, puffer application of AMPA to single HM generates inward currents which, when repeated in the presence of a concentration of DHPG (5 μM) subthreshold to induce oscillations, are followed by repeated oscillations (shown on faster time base in the inset) during the response decay despite the continuous presence of the kainate blocker UBP 301. *B*, on the same cell shown in *A*, after washout of DHPG and return to control conditions, further application of the AMPA receptor antagonist SYM 2206 largely blocks AMPA-evoked currents and prevents the generation of oscillations once DHPG is applied. Holding potential is −60 mV for all traces.

records in Fig. 10*A*) fired irregularly with individual spikes followed by a biphasic pause before the subsequent spike (see right inset for averaged spike from 256 events). Conversely, in an oscillating cell (bottom traces of Fig. 10*A*) spikes were always occurring at the peak of each oscillation, were very regular and followed by a longer pause (see inset on the right; average of 180 events).

On a sample of non-oscillating cells ($n = 9$) the CV for spike firing periodicity was $99 \pm 15\%$, indicating random spike occurrence. In comparison, on oscillating cells ($n = 7$) the CV for spike periodicity was $17 \pm 3\%$. Thus, oscillations determined very regular firing discharges.

An additional property was conferred by DHPG-evoked oscillations as exemplified in Fig. 10*B*. The random firing (CV = 54%) observed at −53 mV in standard saline solution (Fig. 10*B*, top left) was transformed into more regular high frequency firing (CV = 35%) at −40 mV (Fig. 10*B*, bottom left). Conversely, when a neurone was exposed to DHPG and generated oscillations and was kept at a membrane potential (−51 mV) comparable to control, spike generation was not present for each oscillation (Fig. 10*B*, top right), although when it did occur, it was always at the oscillation peak. Further membrane depolarization (−38 mV) increased the number of spikes per oscillation and evoked doublets (interspike interval = 46 ms). Further depolarization to −33 mV generated spike triplets at the peak of oscillations with unchanged frequency (not shown). Thus, cell spiking modality was altered by the DHPG-induced oscillations as spikes could occur only at the peak of oscillations. Furthermore, the average firing rate was constrained by oscillations that limited the incremental rise of firing

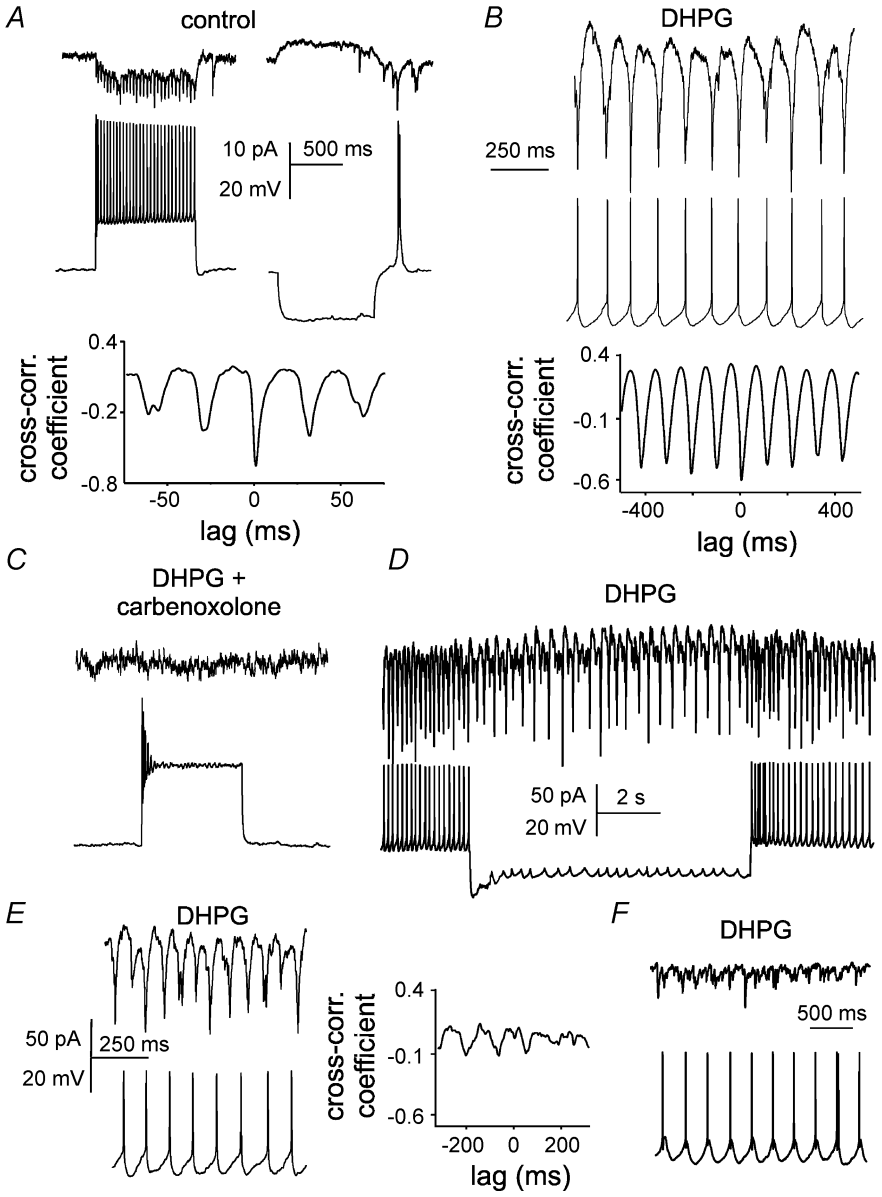

Figure 8. Simultaneous pair recording from HMs reveals their electrical coupling
A, cell 1 (top) under voltage clamp is electrically coupled to cell 2 under current clamp as demonstrated by currents responses elicited in cell 1 by depolarizing or hyperpolarizing changes in membrane potential of cell 2 (0.3 nA injected current of either polarity). As shown in the cross-correlogram (which also includes traces shown above it), responses in both cells were tightly associated (peak occurred near 0 ms) with a small lag between cell 1 and cell 2. *B*, simultaneous slow oscillations present in cell 1 and cell 2 during 25 μM DHPG application. Responses are strongly correlated as indicated by the corresponding plot (which also includes traces shown above it). Same cells as in *A* with the same current and voltage calibrations. *C*, carbenoxolone (100 μM) blocked oscillatory activity in both cells (same pair as in *A* and *B*). Injection of a large depolarizing current (0.6 nA) into cell 2 evoked transient firing in this neurone but no response in cell 1, demonstrating loss of electrical coupling. Calibrations as in *A*. *D*, on a pair of HMs oscillating in the presence of DHPG (25 μM), injection of −0.3 nA steady current into cell 2 slows down oscillatory activity in cell 1, a phenomenon reversible at the end of current injection. *E*, example of pair recording from two HMs oscillating in the presence of DHPG with different oscillatory period (see lack of correlation between such events in the cross-correlogram which also includes traces shown alongside it). *F*, example of pair of cells in which top HM does not oscillate in the presence of DHPG (25 μM) while the bottom one generates repeated slow oscillations. Current and voltage calibrations as in *E*.

versus membrane potential as demonstrated in the plots (Fig. 10*C*) for cells in control saline (■) or in the presence of DHPG-evoked oscillations (□).

Raising extracellular K^+ (7.5–9 mM) induced HM membrane depolarization (from −60 to −52 mV in the example of Fig. 7*D*; -12 ± 2 mV on average; $n = 5$) without oscillations, and it elicited repetitive irregular firing as indicated in the inset to Fig. 10*D*. On average the CV for spike discharges in high external K^+ was $63 \pm 10\%$. Thus, current injection or high K^+ evoked a firing pattern clearly different from the one associated with oscillations.

Finally, we tested if the efficiency of the glutamatergic input to activate HM via the dorso-medullary reticular column (DMRC; Cunningham & Sawchenko, 2000) could be modulated in the presence of DHPG. For such tests we stimulated electrically the DMRC (Sharifullina *et al.* 2004) and used a small subthreshold concentration of DHPG to induce slow oscillations (and associated firing) to avoid them interfering with synaptic processes. Figure 10*E* shows an example in which, in the presence of 5 μM DHPG, after repolarizing the cell membrane potential to the initial resting level (−64 mV), the EPSP could now generate a spike followed (after 184 ± 4 ms delay) by cycles of oscillatory activity (see inset to Fig. 10*E*). Comparable data were observed on five HMs.

Discussion

The principal finding of the present study is the demonstration that, on brainstem motoneurones at early postnatal age, mGluR1s evoked a novel oscillatory (4–8 Hz) activity hitherto unreported on such cells. Oscillations required electrical coupling amongst HMs, and were apparently paced by rhythmic activation of K_{ATP} conductances. Because these oscillations constrained spike firing into a regular mode, they might represent a mechanism to coordinate motor discharges to tongue muscles at a critical stage of neonatal development.

Origin and characteristics of oscillations

Oscillations did not arise spontaneously (even when the network was depolarized by high K^+) and were not a consequence of synaptic inhibition block, as they were

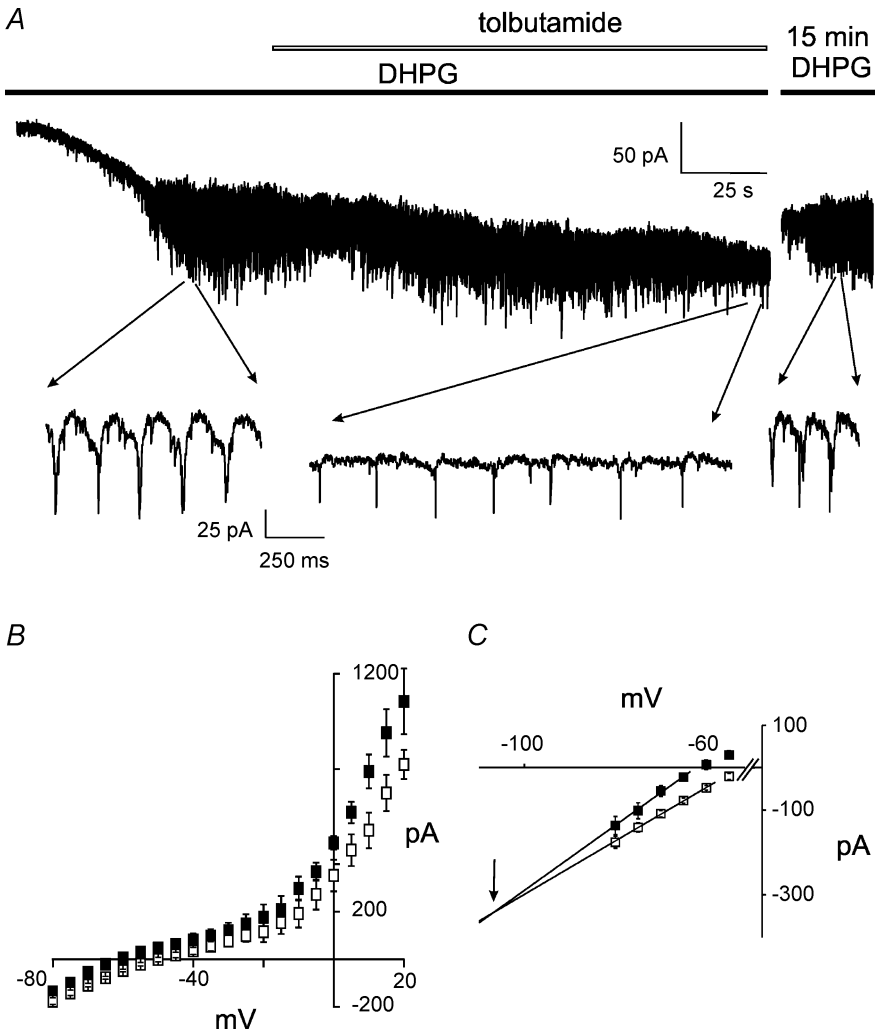

Figure 9. Sulphonylureas block slow oscillations evoked by DHPG
A, DHPG (25 μM) elicits inward current and slow oscillations (see inset with expanded time base). Further application of tolbutamide (500 μM) induces inward current and disrupts slow oscillations while leaving less regular (CV = 36% *versus* 8% prior to tolbutamide) fast discharges (inset, middle). Return of slow oscillations in the continuous presence of DHPG is observed after 15 min washout of tolbutamide (right). *B*, *I–V* plots (produced by 6 s voltage ramps from −80 to +20 mV) obtained during the oscillatory activity induced by DHPG (■) and after application (□) of either glibenclamide (50 μM) or tolbutamide (500 μM). Data with these agents were pooled together. Values are from 12 HMs. *C*, the *I–V* plot of *B* in the region negative to the holding potential is expanded to show decreased slope in the presence of sulphonylureas with extrapolated line crossover at −106 mV as indicated by the arrow.

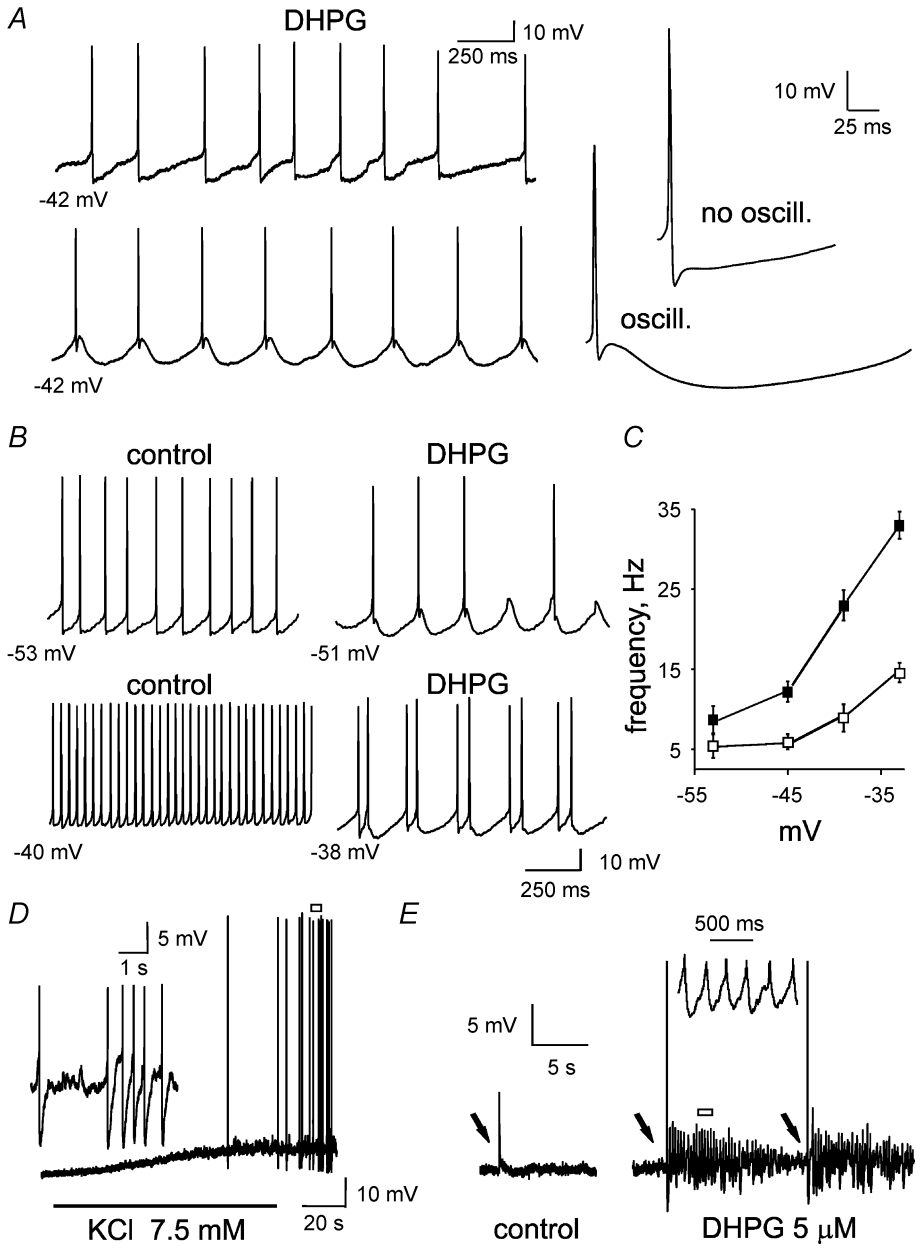

Figure 10. Firing properties of HMs during oscillatory activity evoked by DHPG
A, example of two HMs recorded in the presence of DHPG (25 μM) at the same membrane potential from two different slices. The cell at the top did not generate oscillations and fired randomly. Averaged spike is shown on the right. Bottom is an example of a cell oscillating in DHPG solution and regularly firing (average spike on the right). *B*, comparison of firing properties of a cell in control saline (left; firing irregularly at −53 mV, or at high frequency at −40 mV) with a cell oscillating in DHPG solution (right) with intermittent firing in coincidence with oscillations at −51 mV, or highly regular doublets at −38 mV. *C*, plots of average firing frequency *versus* membrane potential for a sample of 5 HMs in control saline (■) or in DHPG solution (□). Data for control cells were obtained by analysing 10-s-long records while data from DHPG-treated cells were averaged from 5- to 10-s-long records. *D*, application of 7.5 mM K^+ solution depolarizes HM from −61 to −52 mV, and induces irregular firing (see inset where spikes are truncated which corresponds to open horizontal bar). *E*, EPSPs induced by electrical stimulation (0.1 Hz; 0.1 ms; subthreshold for spiking as indicated by arrows) of the DMRC in control solution (left) or in the presence of 5 μM DHPG (middle and right), a concentration subthreshold for generating oscillations. Coincidence of EPSP and DHPG brings about spike generation and oscillations following the synaptic response (see inset for expanded trace corresponding to open horizontal bar). All responses are obtained at −64 mV after injection of steady current to repolarize the cell in the presence of DHPG.

present even in the absence of strychnine and bicuculline. Note that application of the selective $GABA_B$ receptor blocker CGP 55845 did not change oscillations induced by DHPG, suggesting that $GABA_B$ receptors were not involved in oscillations. This result accords with the previous demonstration that, at least at this developmental age, there is no contribution by $GABA_B$ receptors to inhibitory synaptic transmission on rat HMs even during repeated neuronal activity (Donato & Nistri, 2001).

The triggering factor was activation of mGluR1s by DHPG, a selective mGluR1 agonist (Schoepp *et al.* 1999) that generates neuronal depolarization with increased input resistance and enhances glutamatergic transmission (Sharifullina *et al.* 2004) through stimulation of intracellular IP_3 synthesis and Ca^{2+} release (Schoepp *et al.* 1999). These combined effects of DHPG presumably activated premotoneurones at network level to trigger oscillations as demonstrated by the requirement for efficient glutamatergic transmission (via AMPA receptors sensitive to the selective blocker SYM 2206). Oscillations could also arise after activating network neurones with focal pulses of AMPA in the presence of DHPG. Thus, the origin of HM oscillations was based on spike-dependent, Ca^{2+}-mediated release of endogenous glutamate in accordance with the observed block by TTX or Mn^{2+}. Note, however, that once oscillations were developed, there was no rhythmic discharge of glutamatergic premotoneurones because synaptic currents were equally distributed throughout the oscillation cycle, ruling out concerted periodic firing of premotoneurones as the mechanism generating and maintaining oscillations. Thus, enhanced glutamatergic input was necessary to constrain HMs into an oscillatory mode; however, once established, oscillations were crucially dependent on HM collective behaviour.

Although endogenous glutamate can activate different classes of ionotropic receptors, it seems unlikely that NMDA receptors contributed to the recorded oscillations because these responses were insensitive to the selective receptor blocker APV. Furthermore, synaptically released glutamate may also activate kainate receptors which, on cortical neurones, mediate EPSCs characterized by rather slow kinetics (Kidd & Isaac, 2001; Ali, 2003). In the present experiments on DHPG-evoked oscillations, the emergence of slow, large synaptic responses, especially at positive holding potential, may have suggested underlying activation of kainate receptors. Nevertheless, application of the selective kainate receptor antagonist UBP 301 failed to block oscillations as well as the slow, large outward synaptic currents, making it unlikely that kainate receptor activity took part in such oscillations. The predominant role of AMPA receptors activated by endogenous glutamate was further corroborated by the observation that the selective AMPA antagonist SYM 2206 (Behr *et al.* 2002) blocked HM currents induced by puffer-applied AMPA as well as any oscillatory activity evoked by DHPG.

The large, slow outward currents intermingled with oscillations at positive potentials were thus likely to be summated synaptic events due to AMPA receptors because of their SYM 2206 sensitivity. Their slow kinetics at positive potential were shared by AMPA-elicited currents, which exhibited clear outward rectification, probably because they reflected the relative lack of GluR2 subunits in AMPA receptors of HMs (Essin *et al.* 2002), a fact that confers them rectification properties.

It would be inappropriate to consider oscillations as an intrinsic property of individual motoneurones due to cyclic interactions among certain voltage-activated conductances. In fact, on HMs strong buffering of intracellular Ca^{2+} or intracellular application of QX-314 to block Na^+ and I_h currents, or a range of channel inhibitors (Ba^{2+}, apamin, Cs^+, ZD 7288) failed to affect either the amplitude or the period of oscillations, in keeping with the notion that intrinsic membrane conductances of HMs had little effect on the genesis of oscillations. In this sense oscillations of HMs were therefore different from those recorded from other brain neurones in which a role for a variety of voltage-activated ion channels can be demonstrated (Traub *et al.* 2002, 2004). Hence, activation of mGluR1 receptors of brainstem neurones represents a novel and very efficient mechanism to up-regulate cell excitability without interference with major voltage-activated conductances. The amplitude and period of oscillations were also insensitive to membrane potential, suggesting that oscillations recorded from HMs were not just large excitatory synaptic currents.

Electrical coupling amongst HMs is necessary for oscillatory activity and unveils concerted rhythmic behaviour of HMs

In other brain areas, like for example the hippocampus or the thalamus, electrical coupling amongst neurones is an essential process to produce oscillatory activity (Skinner *et al.* 1999; Hughes *et al.* 2002*b*; LeBeau *et al.* 2003; Long *et al.* 2004). Manifestations of such coupling are fast inward currents ('spikelets') and slow bursts ('burstlets') passively propagated from one cell to the next via specialized gap junctions made up of carbenoxolone-sensitive membrane proteins termed connexins (Honma *et al.* 2004) and pannexins (Bruzzone *et al.* 2003). Since early discharges and fast inward currents during slow oscillations of HMs had similar kinetics and pharmacology, it seems likely that they were all spikelets due to repeated firing of HM action potentials.

In accordance with previous studies indicating that a substantial number of rat HMs are electrically coupled (Mazza *et al.* 1992; Rekling *et al.* 2000),

the present investigation, using simultaneous patch recording from HMs, found significant electrical coupling (without rectification) readily blocked by carbenoxolone. Regardless of whether pairs of cells were coupled or not, and on all single-recorded cells, carbenoxolone always suppressed oscillations. These data suggest that spikelets and burstlets making up oscillations were electrically propagated responses generated by cells close to the recorded one, in analogy to the phenomenon described for thalamic neurones (Long *et al.* 2004). Although DHPG application was therefore responsible to spark off HM depolarization, activation of mGluR1s was not apparently accompanied by changes in gap junction efficiency as demonstrated by the preserved value of the electrical coupling coefficient. Since this coupling normally involves a few HMs (Mazza *et al.* 1992), injection of current into one HM could slow down oscillations in the paired recorded cell without fully suppressing oscillations probably still driven by other coupled neurones.

The insensitivity of the oscillation period to membrane potential in a *single* HMs could be explained by the fact that blocking just one HM (and/or its immediate neighbour) could not suppress oscillations propagated by nearby HMs. Likewise, intracellular application of channel blockers to a single cell could not disrupt oscillations as these drugs did not apparently cross to adjacent HMs. In fact, neurobiotin-injected HMs did not show dye coupling despite the presence of oscillations presumably because gap junctions are ill-suited to transport chemical substances (Arabshahi *et al.* 1997; Devor & Yarom, 2002). As far as the locus for electrical coupling among HMs is concerned, the insensitivity of the oscillatory period to active membrane properties of the recorded HM plus the block of oscillations by AMPA antagonists (or the triggering of oscillations by focal pulses of AMPA) all make unlikely an axo-axonic coupling source and rather point to a somato-dendritic location (Honma *et al.* 2004) of gap junctions (Traub *et al.* 2003, 2004). In fact, in hippocampal slice neurones, axo-axonic coupling responsible for spikelets is typically suppressed by somatic membrane hyperpolarization (Schmitz *et al.* 2001), contrary to the findings of the present study. In conclusion, within the nucleus hypoglossus, gap junctions are unlikely to be axo-axonic and appear to tighten the organization of the rhythm rather than generate network oscillations, as in the case of the hippocampus (Draguhn *et al.* 1998; Traub *et al.* 2002).

A mechanism to pace oscillations

A distinguishing feature of HM oscillations was that, in the presence of DHPG, they could last indefinitely as long as recording was possible. While this property rules out mGluR1 desensitization or rundown, it also implies a mechanism to ensure periodicity of oscillations, especially because oscillations could be routinely observed in the presence of synaptic inhibition blockers.

The slow inward current evoked by DHPG was initially associated with a resistance increase presumably due to block of an outward K^+ conductance (Sharifullina *et al.* 2004). Nevertheless, this resistance rise rapidly dissipated once slow oscillations emerged. The simplest interpretation is that emergence of the oscillatory activity coincided not only with depolarization spread via gap junctions but also with activation of a conductance mechanism functionally opposite to the closure of leak channels. Although we cannot exclude the additional contribution by activation of certain voltage-dependent conductances due to current flow from nearby unclamped cells, this hypothesis is made unlikely by the insensitivity of input resistance to large depolarization or hyperpolarization (-80 to $+20$ mV). Pharmacological data on the blocking effect of sulphonylureas instead suggested a different explanation, namely co-activation of an outward K^+ current mediated by K_{ATP} channels to contrast the resistance increase evoked by DHPG, and to arrest oscillations. Because the K_{ATP} conductance targeted by sulphonylureas has relatively modest voltage dependence (Aguilar-Bryan & Bryan, 1999), its sulphonylurea-dependent inhibition during the oscillatory phase is expected to be accompanied by a quasi-parallel downward shift of the cell *I–V* relation, as was indeed found in the present study. Furthermore, in the presence of sulphonylureas slow oscillations were severely disrupted, leaving irregular spikelets. This observation indicates that gap junctions were not blocked by sulphonylureas, even though their synchronizing mechanism had been lost.

On cerebellar granule (D'Angelo *et al.* 2001) or thalamic (Fuentealba *et al.* 2004) neurones, oscillations in the frequency range found on HMs were demonstrated to be paced by cyclic activation of a slow K^+ conductance with kinetics comparable to the slow outward current of HM oscillations. While the precise identification of such a K^+ conductance remains to be established, previous studies have shown that on brainstem respiratory neurones rhythmic changes in K_{ATP} channel activity take place during oscillations presumably because of cyclic variations in the intracellular ATP concentration in the immediate vicinity of the K_{ATP} channels (Haller *et al.* 2001). We suspect that the excitation of HMs set off by DHPG might have been associated with analogous changes in intracellular ATP so that a periodic block/unblock of K_{ATP} channels could occur depending on the energy metabolism of HMs during application of DHPG.

Developmental characteristics of oscillatory mechanisms

In view of the strong developmental regulation of connexins (Honma *et al.* 2004), it seems likely that the

extent of their expression, which is particularly high after birth, was an important element to determine whether HMs could oscillate. In addition, the postnatal period is also associated with major changes in the expression of mGluR1s (Shigemoto *et al.* 1992; Catania *et al.* 1994) and K_{ATP} channels (Mourre *et al.* 1990). Thus, concurrent expression of mGluR1s, connexins and K_{ATP} channels may explain why optimization of HM oscillatory activity had a narrow time window relying on the synergy between these phenomena. It is currently unknown if activation of mGluR1 receptors in the brainstem of the adult rat can generate analogous oscillations. Although HMs gradually change some of their electrical properties during postnatal maturation (Berger *et al.* 1996), it is clear that certain characteristics such as those of gap junctions (Ramirez *et al.* 1997; Simbürger *et al.* 1997) and responsiveness to K_{ATP} channel blockers are retained (Pierrefiche *et al.* 1997), suggesting that at least in principle activation of mGluR1 receptors might generate fast oscillations which might participate in certain fast discharges normally recorded from the adult hypoglossal nerve *in vivo* (O'Neal III *et al.* 2004). This issue will, however, require future experiments to investigate the role of mGluR1 receptors in the adult brainstem.

Oscillations are due to the interplay amongst HM conductances

mGluR-dependent theta (4–12 Hz) oscillations of hippocampal pyramidal cells possess distinctive properties like dependence on GABA-mediated inhibition, requirement of AMPA receptor block, and out of phase discharge of inhibitory interneurones (Traub *et al.* 2004), indicating cellular mechanisms distinct from those of HM oscillations.

On certain reticulothalamic neurones theta oscillations are induced by mGluR1 activation with characteristics similar to those of HMs, including strong dependence on gap junctions (Hughes *et al.* 2004). There are, however, a few properties which make such theta oscillations different from those of HMs: for instance, thalamic oscillations persist in the presence of TTX and require intact GABAergic transmission (Hughes *et al.* 2004).

We might envisage the following scenario for the 4–8 Hz oscillations recorded from HMs: even in the absence of synaptic inhibition, oscillations started because of DHPG-enhanced glutamatergic transmission at network level, and were amplified by the associated resistance increase in premotoneurones and HMs. Network glutamatergic activity (evoked by DHPG) could lead to repeated HM firing sensitive to TTX and manifested as spikelets which are believed to be individual spikes electrotonically spread via gap junctions (Hughes *et al.* 2002*a*, 2004; Long *et al.* 2004).

HMs possess comparatively large intracellular levels of free Ca^{2+} (Ladewig & Keller, 2000) and generate long lasting increases in intracellular Ca^{2+} even after a single action potential (Donato *et al.* 2003). Intracellular Ca^{2+} homeostasis in brain neurones is largely dependent on the operation of the Ca^{2+}-ATPase pump expected to consume a significant concentration of intracellular ATP (Watson *et al.* 2003). Release of intracellular Ca^{2+} from organelle stores after application of DHPG (Schoepp *et al.* 1999) plus lingering intracellular Ca^{2+} due to repeated spikes might have therefore cooperated to induce strong operation of the Ca^{2+} pump and depleted ATP with consequent activation of K_{ATP} channels to hyperpolarize HMs (burstlets). The interplay among these mechanisms might have presumably established the conditions necessary for the cyclic waxing and waning of the depolarization cycle propagated and synchronized across gap junctions.

Firing characteristics during oscillations

Current clamp experiments demonstrated that the emergence of oscillations conferred important properties to the firing characteristics of HMs. While rhythmic oscillations of respiratory neurones are believed to facilitate spike firing (Parkis *et al.* 2003), for HMs the main consequence was transformation of irregular firing, often at high rate, into a regular, lower frequency discharge. Because the oscillatory period was little dependent on membrane voltage, the overall spike output of the cell was constrained to the number of oscillatory cycles. Even if, at more depolarized level of membrane potential, oscillations could generate doublets or triplets of action potentials, the remarkable consequence of oscillations was the emergence of low rhythmic firing. This phenomenon might even represent a braking system to avoid excessive excitation of HMs which are particularly vulnerable to large elevations in intracellular Ca^{2+} and excitotoxic damage (Ladewig *et al.* 2003).

A brain slice preparation is ill suited to investigate the role of projection pathways because many connections are inevitably severed. Nevertheless, in the brainstem slice preparation it is possible to preserve a strong glutamatergic input from the DMRC to HMs (Cunningham & Sawchenko, 2000). In the present experiments electrical stimulation of this pathway in association with a DHPG concentration subthreshold for oscillations, facilitated EPSP–spike coupling and elicited a set of oscillations for each synaptic stimulus. These data suggest that it was not necessary to apply DHPG in very large concentrations to enhance firing and generate oscillations.

Functional implications

HMs receive rhythmic synaptic inputs from a variety of brainstem networks which include oscillators for respiration, swallowing, mastication, etc. (Nakamura *et al.* 1999; Jean, 2001; Ballanyi, 2004). As far as respiratory rhythms transmitted to the hypoglossal nucleus are

concerned, in the adult as well as neonate rat *in vivo*, inspiratory discharges occur at about 1–2 Hz (Thomas & Marshall, 1997) with superimposed much faster oscillations, whose frequency increases during development (Kocsis *et al.* 1999; Marchenko *et al.* 2002). Pioneer work by Suzue (1984) has demonstrated that isolated brainstem preparations retain rhythmic activities although at lower frequency probably because of the different experimental conditions (including the use of ambient temperature and severance of peripheral afferents). The spontaneous inspiratory rhythm of the isolated brainstem preparation recorded from the rat hypoglossus nerve *in vitro* has about 0.1 Hz frequency (Morin *et al.* 1992), but it can be readily accelerated by serotonin (Morin *et al.* 1992) or high K^+, or largely slowed down by hypoxia (Ballanyi, 2004). While HMs within the thin brainstem slice preparation showed no spontaneous rhythmic activity, application of DHPG persistently increases their synaptic inputs in a dose-dependent fashion (Sharifullina *et al.* 2004), showing that the effect of DHPG goes in the opposite direction of the anoxic response (Ballanyi, 2004). Thus, there is no evidence that the oscillations induced by DHPG on *in vitro* HMs were the expression of a pathophysiological effect. On the contrary, the fast oscillations evoked by DHPG at room temperature were approaching the frequency range (22–43 Hz) normally found for medium frequency oscillations superimposed on the inspiratory discharges of the newborn rat *in vivo* (Kocsis *et al.* 1999). Although pattern similarity cannot indicate equivalence of function, these data suggest that oscillations as fast as those evoked by DHPG might also be expressed by *in vivo* brainstem neurones. The frequency of slow oscillations (about 6 Hz) induced by DHPG would be too fast for the normal inspiratory rhythm of *in vivo* normoxic animals, but it could correspond to reflex-enhanced respiratory rhythmicity especially because mGluRs are believed to increase the respiratory frequency even if they are not usually active in eupnoea (Li & Nattie, 1995). Furthermore, since application of DHPG facilitated synaptic inputs from the DMRC, a structure regarded as particularly important for swallowing (Cunningham & Sawchenko, 2000), it is feasible that activation of mGluR1s on brainstem neurones might represent a global strategy to facilitate HM rhythmic firing to tongue muscles under high demand-led conditions set by brainstem networks like, for instance, during suckling behaviour (Berger *et al.* 1996). *In vivo* experiments will, however, be necessary to clarify the role of mGluRs in the complex functions mediated by HMs.

References

Aguilar-Bryan L & Bryan J (1999). Molecular biology of adenosine triphosphate-sensitive potassium channels. *Endocr Rev* **20**, 101–135.

Ali A (2003). Involvement of post-synaptic kainate receptors during synaptic transmission between unitary connections in rat neocortex. *Eur J Neurosci* **17**, 2344–2350.

Arabshahi A, Giaume C & Peusner KD (1997). Lack of biocytin transfer at gap junctions in the chicken vestibular nuclei. *Int J Dev Neurosci* **15**, 343–352.

Ashcroft FM (1988). Adenosine 5′-triphosphate-sensitive potassium channels. *Annu Rev Neurosci* **11**, 97–118.

Ballanyi K (2004). Protective role of neuronal K_{ATP} channels in brain hypoxia. *J Exp Biol* **207**, 3201–3212.

Behr J, Gebhardt C, Heinemann U & Mody I (2002). Kindling enhances kainate receptor-mediated depression of GABAergic inhibition in rat granule cells. *Eur J Neurosci* **16**, 861–867.

Beierlein M, Gibson JR & Connors BW (2000). A network of electrically coupled interneurons drives synchronized inhibition in neocortex. *Nat Neurosci* **3**, 904–910.

Berger AJ, Bayliss DA & Viana F (1996). Development of hypoglossal motoneurons. *J Appl Physiol* **81**, 1039–1048.

Bruzzone R, Hormuzdi SG, Barbe MT, Herb A & Monyer H (2003). Pannexins, a family of gap junction proteins expressed in brain. *Proc Natl Acad Sci U S A* **100**, 13644–13649.

Catania MV, Landwehrmeyer GB, Testa CM, Standaert DG, Penney JB Jr & Young AB (1994). Metabotropic glutamate receptors are differentially regulated during development. *Neuroscience* **61**, 481–495.

Cobb SR, Bulters DO & Davies CH (2000). Coincident activation of mGluRs and mAChRs imposes theta frequency patterning on synchronised network activity in the hippocampal CA3 region. *Neuropharmacology* **39**, 1933–1942.

Cunningham ET Jr & Sawchenko PE (2000). Dorsal medullary pathways subserving oromotor reflexes in the rat: implications for the central neural control of swallowing. *J Comp Neurol* **417**, 448–466.

D'Angelo E, Nieus T, Maffei A, Armano S, Rossi P, Taglietti V, Fontana A & Naldi G (2001). Theta-frequency bursting and resonance in cerebellar granule cells: experimental evidence and modeling of a slow K^+-dependent mechanism. *J Neurosci* **21**, 759–770.

Devor A & Yarom Y (2002). Electrotonic coupling in the inferior olivary nucleus revealed by simultaneous double patch recordings. *J Neurophysiol* **87**, 3048–3058.

Donato R, Canepari M, Lape R & Nistri A (2003). Effects of caffeine on the excitability and intracellular Ca^{2+} transients of neonatal rat hypoglossal motoneurons in vitro. *Neurosci Lett* **346**, 177–181.

Donato R & Nistri A (2000). Relative contribution by GABA or glycine to Cl^--mediated synaptic transmission on rat hypoglossal motoneurons in vitro. *J Neurophysiol* **84**, 2715–2724.

Donato R & Nistri A (2001). Differential short-term changes in GABAergic or glycinergic synaptic efficacy on rat hypoglossal motoneurons. *J Neurophysiol* **86**, 565–574.

Draguhn A, Traub RD, Schmitz D & Jefferys JG (1998). Electrical coupling underlies high-frequency oscillations in the hippocampus in vitro. *Nature* **394**, 189–192.

Essin K, Nistri A & Magazanik L (2002). Evaluation of GluR2 subunit involvement in AMPA receptor function of neonatal rat hypoglossal motoneurons. *Eur J Neurosci* **15**, 1899–1906.

Fuentealba P, Timofeev I & Steriade M (2004). Prolonged hyperpolarizing potentials precede spindle oscillations in the thalamic reticular nucleus. *Proc Natl Acad Sci U S A* **101**, 9816–9821.

Galarreta M & Hestrin S (1999). A network of fast-spiking cells in the neocortex connected by electrical synapses. *Nature* **402**, 72–75.

Grillner S, Ekeberg El Manira A, Lansner A, Parker D, Tegner J & Wallen P (1998). Intrinsic function of a neuronal network – a vertebrate central pattern generator. *Brain Res Rev* **26**, 184–197.

Haller M, Mironov SL, Karschin A & Richter DW (2001). Dynamic activation of K_{ATP} channels in rhythmically active neurons. *J Physiol* **537**, 69–81.

Hay M, McKenzie H, Lindsley K, Dietz N, Bradley SR, Conn PJ & Hasser EM (1999). Heterogeneity of metabotropic glutamate receptors in autonomic cell groups of the medulla oblongata of the rat. *J Comp Neurol* **403**, 486–501.

Honma S, De S, Li D, Shuler CF & Turman JE Jr (2004). Developmental regulation of connexins 26, 32, 36, and 43 in trigeminal neurons. *Synapse* **52**, 258–271.

Hughes SW, Blethyn KL, Cope DW & Crunelli V (2002*a*). Properties and origin of spikelets in thalamocortical neurones in vitro. *Neuroscience* **110**, 395–401.

Hughes SW, Cope DW, Blethyn KL & Crunelli V (2002*b*). Cellular mechanisms of the slow (<1 Hz) oscillation in thalamocortical neurons in vitro. *Neuron* **33**, 947–958.

Hughes SW, Lorincz M, Cope DW, Blethyn KL, Kekesi KA, Parri HR, Juhasz G & Crunelli V (2004). Synchronized oscillations at alpha and theta frequencies in the lateral geniculate nucleus. *Neuron* **42**, 253–268.

Jean A (2001). Brain stem control of swallowing: neuronal network and cellular mechanisms. *Physiol Rev* **81**, 929–969.

Kidd F & Isaac J (2001). Kinetics and activation of postsynaptic kainate receptors at thalamocortical synapses: role of glutamate clearance. *J Neurophysiol* **86**, 1139–1148.

Kiehn O, Kjaerulff O, Tresch MC & Harris-Warrick RM (2000). Contributions of intrinsic motor neuron properties to the production of rhythmic motor output in the mammalian spinal cord. *Brain Res Bull* **53**, 649–659.

Kirk IJ & Mackay JC (2003). The role of theta-range oscillations in synchronising and integrating activity in distributed mnemonic networks. *Cortex* **39**, 993–1008.

Kocsis B, Gyimesi-Pelczer K & Vertes RP (1999). Medium-frequency oscillations dominate the inspiratory nerve discharge of anesthetized newborn rats. *Brain Res* **818**, 180–183.

Ladewig T & Keller BU (2000). Simultaneous patch-clamp recording and calcium imaging in a rhythmically active neuronal network in the brainstem slice preparation from mouse. *Pflugers Arch* **440**, 322–332.

Ladewig T, Kloppenburg P, Lalley PM, Zipfel WR, Webb WW & Keller BU (2003). Spatial profiles of store-dependent calcium release in motoneurones of the nucleus hypoglossus from newborn mouse. *J Physiol* **547**, 775–787.

Landisman CE, Long MA, Beierlein M, Deans MR, Paul DL & Connors BW (2002). Electrical synapses in the thalamic reticular nucleus. *J Neurosci* **22**, 1002–1009.

Lape R & Nistri A (2001). Characteristics of fast Na^+ current of hypoglossal motoneurons in a rat brainstem slice preparation. *Eur J Neurosci* **13**, 763–772.

LeBeau FE, Traub RD, Monyer H, Whittington MA & Buhl EH (2003). The role of electrical signaling via gap junctions in the generation of fast network oscillations. *Brain Res Bull* **62**, 3–13.

Leznik E, Makarenko V & Llinas R (2002). Electrotonically mediated oscillatory patterns in neuronal ensembles: an in vitro voltage-dependent dye-imaging study in the inferior olive. *J Neurosci* **22**, 2804–2815.

Li A & Nattie EE (1995). Prolonged stimulation of respiration by brain stem metabotropic glutamate receptors. *J Appl Physiol* **79**, 1650–1656.

Long MA, Landisman CE & Connors BW (2004). Small clusters of electrically coupled neurons generate synchronous rhythms in the thalamic reticular nucleus. *J Neurosci* **24**, 341–349.

Marchenko V, Granata AR & Cohen MI (2002). Respiratory cycle timing and fast inspiratory discharge rhythms in the adult decerebrate rat. *Am J Physiol Regul Integr Comp Physiol* **283**, R931–940.

Marchetti C, Pagnotta S, Donato R & Nistri A (2002). Inhibition of spinal or hypoglossal motoneurons of the newborn rat by glycine or GABA. *Eur J Neurosci* **15**, 975–983.

Marchetti C, Taccola G & Nistri A (2003). Distinct subtypes of group I metabotropic glutamate receptors on rat spinal neurons mediate complex facilitatory and inhibitory effects. *Eur J Neurosci* **18**, 1873–1883.

Mazza E, Nunez-Abades PA, Spielmann JM & Cameron WE (1992). Anatomical and electrotonic coupling in developing genioglossal motoneurons of the rat. *Brain Res* **598**, 127–137.

More J, Troop H, Dolman N & Jane D (2003). Structural requirements for novel willardiine derivatives acting as AMPA and kainate receptor antagonists. *Br J Pharmacol* **138**, 1093–1100.

Morin D, Monteau R & Hilaire G (1992). Compared effects of serotonin on cervical and hypoglossal inspiratory activities: an in vitro study in the newborn rat. *J Physiol* **451**, 605–629.

Mourre C, Widmann C & Lazdunski M (1990). Sulfonylurea binding sites associated with ATP-regulated K^+ channels in the central nervous system: autoradiographic analysis of their distribution and ontogenesis, and of their localization in mutant mice cerebellum. *Brain Res* **519**, 29–43.

Nakamura Y, Katakura N & Nakajima M (1999). Generation of rhythmical ingestive activities of the trigeminal, facial, and hypoglossal motoneurons in in vitro CNS preparations isolated from rats and mice. *J Med Dent Sci* **46**, 63–73.

O'Neal MH III, Spiegel ET, Chon KH & Solomon IC (2004). Time-frequency representation of inspiratory motor output in anesthetized C57BL/6 mice in vivo. *J Neurophysiol*; DOI:10.1152/jn.00646.2004.

Oyamada Y, Andrzejewski M, Muckenhoff K, Scheid P & Ballantyne D (1999). Locus coeruleus neurones in vitro: pH-sensitive oscillations of membrane potential in an electrically coupled network. *Respir Physiol* **118**, 131–147.

Parkis MA, Feldman JL, Robinson DM & Funk GD (2003). Oscillations in endogenous inputs to neurons affect excitability and signal processing. *J Neurosci* **23**, 8152–8158.

Perez Velazquez JL & Carlen PL (2000). Gap junctions, synchrony and seizures. *Trends Neurosci* **23**, 68–74.

Pierrefiche O, Bischoff AM, Richter DW & Spyer KM (1997). Hypoxic response of hypoglossal motoneurones in the in vivo cat. *J Physiol* **15**, 785–795.

Ramirez JM, Quellmalz UJ & Wilken B (1997). Developmental changes in the hypoxic response of the hypoglossus respiratory motor output in vitro. *J Neurophysiol* **78**, 383–392.

Rekling JC, Shao XM & Feldman JL (2000). Electrical coupling and excitatory synaptic transmission between rhythmogenic respiratory neurons in the preBotzinger complex. *J Neurosci* **20**, RC113.

Rybak IA, Shevtsova NA, St John WM, Paton JF & Pierrefiche O (2003). Endogenous rhythm generation in the pre-Botzinger complex and ionic currents: modelling and in vitro studies. *Eur J Neurosci* **18**, 239–257.

Schmidt BJ, Hochman S & MacLean JN (1998). NMDA receptor-mediated oscillatory properties: potential role in rhythm generation in the mammalian spinal cord. *Ann N Y Acad Sci* **860**, 189–202.

Schmitz D, Schuchmann S, Fisahn A, Draguhn A, Buhl EH, Petrasch-Parwez E, Dermietzel R, Heinemann U & Traub RD (2001). Axo-axonal coupling a novel mechanism for ultrafast neuronal communication. *Neuron* **31**, 831–840.

Schoepp DD, Jane DE & Monn JA (1999). Pharmacological agents acting at subtypes of metabotropic glutamate receptors. *Neuropharmacology* **38**, 1431–1476.

Sharifullina E, Ostroumov K & Nistri A (2004). Activation of group I metabotropic glutamate receptors enhances efficacy of glutamatergic inputs to neonatal rat hypoglossal motoneurons in vitro. *Eur J Neurosci* **20**, 1245–1254.

Shigemoto R, Nakanishi S & Mizuno N (1992). Distribution of the mRNA for a metabotropic glutamate receptor (mGluR1) in the central nervous system: an in situ hybridization study in adult and developing rat. *J Comp Neurol* **322**, 121–135.

Simbürger E, Stang A, Kremer M & Dermietzel R (1997). Expression of connexin43 mRNA in adult rodent brain. *Histochem Cell Biol* **107**, 127–137.

Skinner FK, Zhang L, Velazquez JL & Carlen PL (1999). Bursting in inhibitory interneuronal networks: a role for gap-junctional coupling. *J Neurophysiol* **81**, 1274–1283.

Steriade M & Timofeev I (2003). Neuronal plasticity in thalamocortical networks during sleep and waking oscillations. *Neuron* **37**, 563–576.

Suzue T (1984). Respiratory rhythm generation in the in vitro brain stem–spinal cord preparation of the neonatal rat. *J Physiol* **354**, 173–183.

Thomas T & Marshall JM (1997). The roles of adenosine in regulating the respiratory and cardiovascular systems in chronically hypoxic, adult rats. *J Physiol* **501**, 439–447.

Towers S, LeBeau F, Gloveli T, Traub RD, Whittington MA & Buhl EH (2002). Fast network oscillations in the rat dentate gyrus in vitro. *J Neurophysiol* **87**, 1165–1168.

Traub RD, Bibbig A, LeBeau FE, Buhl EH & Whittington MA (2004). Cellular mechanisms of neuronal population oscillations in the hippocampus in vitro. *Annu Rev Neurosci* **27**, 247–278.

Traub RD, Draguhn A, Whittington MA, Baldeweg T, Bibbig A, Buhl EH & Schmitz D (2002). Axonal gap junctions between principal neurons: a novel source of network oscillations, and perhaps epileptogenesis. *Rev Neurosci* **13**, 1–30.

Traub RD, Pais I, Bibbig A, LeBeau FE, Buhl EH, Hormuzdi SG, Monyer H & Whittington MA (2003). Contrasting roles of axonal (pyramidal cell) and dendritic (interneuron) electrical coupling in the generation of neuronal network oscillations. *Proc Natl Acad Sci U S A* **100**, 1370–1374.

Watson WD, Facchina SL, Grimaldi M & Verma A (2003). Sarco-endoplasmic reticulum Ca^{2+} ATPase (SERCA) inhibitors identify a novel calcium pool in the central nervous system. *J Neurochem* **87**, 30–43.

Whittington MA, Traub RD & Jefferys JG (1995). Synchronized oscillations in interneuron networks driven by metabotropic glutamate receptor activation. *Nature* **373**, 612–615.

Wu N, Hsiao CF & Chandler SH (2001). Membrane resonance and subthreshold membrane oscillations in mesencephalic V neurons: participants in burst generation. *J Neurosci* **21**, 3729–3739.

Acknowledgements

This work was supported by a FIRB grant.